CFD simulation of neutral ABL flows

Zhang, Xiaodong

Publication date:
2009

Document Version
Publisher's PDF, also known as Version of record

Risø DTU
National Laboratory
for Sustainable Energy

Risø-R-Report

CFD simulation of neutral ABL flows

Xiaodong Zhang

Risø-R-1688(EN)

Risø National Laboratory for Sustainable Energy
Technical University of Denmark
Roskilde, Denmark
April 2009

Author: Xiaodong Zhang
Title: CFD simulation of neutral ABL flows
Division: Aero-elastic Design – Wind Energy Division

Risø-R-1688(EN)
April 2009

Abstract:

This work is to evaluate the CFD prediction of Atmospheric Boundary Layer flow field over different terrains employing Fluent 6.3 software. How accurate the simulation could achieve depend on following aspects: viscous model, wall functions, agreement of CFD model with inlet wind velocity profile and top boundary condition. Fluent employ wall function roughness modifications based on data from experiments with sand grain roughened pipes and channels, describe wall adjacent zone with Roughness Height (Ks) instead of Roughness Length (z_0). In a CFD simulation of ABL flow, the mean wind velocity profile is generally described with either a logarithmic equation by the presence of aerodynamic roughness length z_0 or an exponential equation by the presence of exponent. As indicated by some former researchers, the disagreement between wall function model and ABL velocity profile description will result in some undesirable gradient along flow direction. There are some methods to improve the simulation model in literatures, some of them are discussed in this report, but none of those remedial methods are perfect to eliminate the streamwise gradients in mean wind speed and turbulence, as EllipSys3D could do. In this paper, a new near wall treatment function is designed, which, in some degree, can correct the horizontal gradients problem.
Based on the corrected model constants and near wall treatment function, a simulation of Askervein Hill is carried out. The wind condition is neutrally stratified ABL and the measurements are best documented until now. Comparison with measured data shows that the CFD model can well predict the velocity field and relative turbulence kinetic energy field.
Furthermore, a series of artificial complex terrains are designed, and some of the main simulation results are reported.

ISSN 0106-2840
ISBN 978-87-550-3743-4

Contract no.:

Group's own reg. no.:

Sponsorship:

Cover :

Pages:40
Tables:7
References:19

Information Service Department
Risø National Laboratory for Sustainable Energy
Technical University of Denmark
P.O.Box 49
DK-4000 Roskilde
Denmark
Telephone +45 46774004
bibl@risoe.dk
Fax +45 46774013
www.risoe.dtu.dk

Contents

1 Introduction

Accurate Computational Fluid Dynamics (CFD) simulations of Atmospheric Boundary Layer (ABL) flow over complex terrains are essential for optimization of wind farm micro-siting, as well as for other wind engineering fields, such as prediction of dispersion of pollutants in the atmosphere, prediction of wind load on structure, analysis of wind flow patterns in urban area and constructions siting, etc. The ABL is the lowest part of the atmosphere that is in direct vicinity of earth's surface, its' flow pattern is mostly influenced by ground surface friction and heating or cooling, and its prominent characteristics is turbulence. In fact, the top of ABL could be defined where turbulence disappears. Beyond the top of ABL is geostrophic wind which is controlled by Carioles' force and pressure gradient force and could be treated as laminar flow.

There are comprehensive literatures dealt with CFD simulation of ABL flow over different terrains. Most studies use Reynolds Averaged Navier-Stokes (RANS) equations along with k-ε 2-equation turbulence model and wall functions to calculate near wall parameters. Recently, more and more research employ Large Eddy Simulation (LES) model to try to improve accuracy and illustrate transient wind circulation in lee side of hills or buildings[1], but this transient model is much more time consuming and until now, is not suitable for engineering simulation. The simplicity, robustness and computational economy of the conventional RANS methods have not been seriously challenged by any other turbulence models[2].

In a CFD simulation, the inlet boundary conditions of mean wind speed and turbulence quantities should represent the coming fully developed wind flow, a vertically logarithmic distribution of mean wind speed characteristic with friction velocity u^* and aerodynamic roughness length z_0 is mainly adopted, if the wind is coming from a uniform flat terrain, then the velocity as well as turbulence quantities distribution should not change along the same flat terrain in a suitable CFD simulation model, the streamwise gradients in the vertical profiles of mean wind velocity and turbulence quantities should be zero, this requirement is referred as horizontally homogeneous ABL flow over uniformly rough terrain, and then a flat terrain is a tool to detect disagreements between boundary wind profile and CFD models, especially the viscous model and near wall treatment functions which represent the actual ground surface roughness[3, 4]. Bert Blocken [5, 6] , etc. reported the difficulties some literature encountered to get horizontal homogeneity, concluded that the horizontal variance partially comes from the disagreement between standard wall functions with a sand-grain-based roughness height modification in some commercial CFD codes and ABL profiles characterized with aerodynamic roughness length. Some remedial methods were provided in literatures, but still with limitations to be adopted in simulation of complex terrains. The present paper study the agreement of CFD model with ABL profiles first, and provided a set of newly designed near wall treatment functions as a remediation to partially correct the horizontal gradients problem.

The best known and most comprehensive ABL flow measurements data available is from the Askervein Hill project (P. A. Taylor and H. W. Teunissen, 1983, 1985), which includes two experimental campaigns carried out by an international team. From then on, many studies were focused on the replication of the measurements with CFD simulations [7-9], reference [2] gave a review about turbulence models and near wall treatments in CFD for wind flow over different terrains, such as hills or urban areas. Even so, there is still expensive space to make improvements. This paper carried out a case study of Askervein Hill terrain with a CFD model based on commercial software and adjusted through flat terrain tests. The study show that, compare with some reference works, the present CFD model could produce satisfied

results, especially for the points above the top of the hill. Because roughness conditions are seldom uniform along a spacious ground, a simulation with changing roughness is carried out too.
Askervein Hill is far from steep. An artificial hat place terrain is designed with different steep gradients. Those terrains are useful to compare different CFD models for separation, recirculation, etc. the simulation results from the commercial CFD code Fluent are reported.

2 Fundamental mathematical models

2.1 RANS equations and *k*-ε two-equation turbulence model

Reynolds-Averaged Navier-Stokes equations are written below in Cartesian coordinate[10]:

$$\frac{\partial \rho}{\partial t} + \frac{\partial}{\partial x_i}(\rho u_i) = 0 \tag{1}$$

$$\frac{\partial}{\partial t}(\rho u_i) + \frac{\partial}{\partial x_j}(\rho u_i u_j) = -\frac{\partial p}{\partial x_i} + \frac{\partial}{\partial x_j}\left[\mu\left(\frac{\partial u_i}{\partial x_j} + \frac{\partial u_j}{\partial x_i} - \frac{2}{3}\delta_{ij}\frac{\partial u_l}{\partial x_l}\right)\right] + \frac{\partial}{\partial x_j}\left(-\rho\overline{u_i' u_j'}\right) \tag{2}$$

Where (1) is continuity equation, (2) are momentum equations, u is ensemble-average velocity, $-\rho\overline{u_i' u_j'}$ are Reynolds stress which must be modelled. The standard *k*-ε model assumed that the flow is fully developed turbulence, for ABL that is fully aerodynamically rough, the shear stresses are dominated by Reynolds stresses, and the effects of molecular viscosity are negligible. In incompressible air flow, Reynolds stress is modelled as[11]:

$$-\rho\overline{u_i' u_j'} = \mu_t\left(\frac{\partial u_i}{\partial x_j} + \frac{\partial u_j}{\partial x_i}\right) \tag{3}$$

In *k*-ε model, 2 additional transport equations are solved to calculate the turbulent viscosity μ_t, they are for the turbulence kinetic energy *k* and turbulence dissipation rate ε, in neutral stratification, incompressible air flow without buoyancy effects, they were written as:

$$\frac{\partial}{\partial t}(\rho k) + \frac{\partial}{\partial x_i}(\rho k u_i) = \frac{\partial}{\partial x_j}\left[\left(\mu + \frac{\mu_t}{\sigma_k}\right)\frac{\partial k}{\partial x_j}\right] + P_k - \rho\varepsilon \tag{4}$$

$$\frac{\partial}{\partial t}(\rho \varepsilon) + \frac{\partial}{\partial x_i}(\rho \varepsilon u_i) = \frac{\partial}{\partial x_j}\left[\left(\mu + \frac{\mu_t}{\sigma_\varepsilon}\right)\frac{\partial \varepsilon}{\partial x_j}\right] + C_{1\varepsilon}\frac{\varepsilon}{k}P_k - C_{2\varepsilon}\rho\frac{\varepsilon^2}{k} \tag{5}$$

Where σ_k , $C_{1\varepsilon}$ and $C_{2\varepsilon}$ are model constants, P_k represents the production of turbulence kinetic energy, it is evaluated in *k*-ε model with $P_k = \mu_t S^2$, where $S = \sqrt{2S_{ij}S_{ij}}$ is the modulus of the mean rate-of-strain tensor, $S_{ij} = \frac{1}{2}\left(\frac{\partial u_i}{\partial x_j} + \frac{\partial u_j}{\partial x_i}\right)$, in Cartesian coordinates, it could be write as

$$S_{ij} = \frac{1}{2}\begin{pmatrix} 2\frac{\partial u}{\partial x} & \frac{\partial u}{\partial y}+\frac{\partial v}{\partial x} & \frac{\partial u}{\partial z}+\frac{\partial w}{\partial x} \\ \frac{\partial v}{\partial x}+\frac{\partial u}{\partial y} & 2\frac{\partial v}{\partial y} & \frac{\partial v}{\partial z}+\frac{\partial w}{\partial y} \\ \frac{\partial w}{\partial x}+\frac{\partial u}{\partial z} & \frac{\partial w}{\partial y}+\frac{\partial v}{\partial z} & 2\frac{\partial w}{\partial z} \end{pmatrix} \tag{6}$$

In standard k-ε model, turbulent viscosity is calculated by k and ε as

$$\mu_t = \rho C_\mu \frac{k^2}{\varepsilon} \tag{7}$$

Where C_μ is a model constant with a commonly accepted value of 0.09 in industrial CFD simulation and 0.03 for ABL flow. In a flat terrain ABL flow, a smaller C_μ means that, with stated turbulence intensity, the momentum transport is weaker, the gradient of mean velocity along height is larger. k-ε model is a half empirical turbulence model, C_μ should be adjusted according to measurements.

Consider a flat terrain ABL flow which is steady, incompressible ($\rho = 0, \frac{\partial u_i}{\partial x_i} = 0$), two-dimensional ($v$ =0, w =0, $\frac{\partial u}{\partial y} = 0$), high Reynolds number ($\mu << \mu_t$), no buoyancy and streamwise homogenous ($\frac{\partial u}{\partial x} = 0, \frac{\partial k}{\partial x} = 0, \frac{\partial \varepsilon}{\partial x} = 0$), then the transport equations of kinetic energy and dissipation rate of kinetic energy become

$$0 = \frac{\partial}{\partial z}\left[\frac{\mu_t}{\sigma_k}\frac{\partial k}{\partial z}\right] + P_k - \rho\varepsilon \tag{8}$$

$$0 = \frac{\partial}{\partial z}\left[\frac{\mu_t}{\sigma_\varepsilon}\frac{\partial \varepsilon}{\partial z}\right] + C_{1\varepsilon}\frac{\varepsilon}{k}P_k - C_{2\varepsilon}\rho\frac{\varepsilon^2}{k} \tag{9}$$

Under the above mentioned condition, in the rate-of-strain tensor S_{ij}, only $\frac{\partial u}{\partial z} \neq 0$, $S_{ij}S_{ij} = S_{13}S_{13} + S_{31}S_{31} = 2\left(\frac{1}{2}\frac{\partial u}{\partial z}\right)^2 \Rightarrow S = \sqrt{2S_{ij}S_{ij}} = \frac{\partial u}{\partial z}$, then

$$P_k = \mu_t S^2 = \mu_t\left(\frac{\partial u}{\partial z}\right)^2 \tag{10}$$

The RANS equations could be simplified as

$$\frac{\partial}{\partial x_j}\left(u_j\right) = 0 \tag{11}$$

$$\frac{\partial p}{\partial x} = \frac{\partial}{\partial z}\left(\left(\mu + \mu_t\right)\left(\frac{\partial u}{\partial z}\right)\right) \approx \frac{\partial}{\partial z}\left(\mu_t\left(\frac{\partial u}{\partial z}\right)\right) \tag{12}$$

$$\frac{\partial p}{\partial y} = \frac{\partial p}{\partial z} = 0 \tag{13}$$

The simplification process of momentum equations is given as following. In the equation for momentum balance in x direction, the convective term is

$$\frac{\partial}{\partial x_j}\left(\rho u u_j\right)=\frac{\partial}{\partial x}\left(\rho u u\right)+\frac{\partial}{\partial y}\left(\rho u v\right)+\frac{\partial}{\partial z}\left(\rho u z\right)=0$$

The molecular diffusion term is

$$\frac{\partial}{\partial x_j}\left[\mu\left(\frac{\partial u}{\partial x_j}+\frac{\partial u_j}{\partial x}-\frac{2}{3}\delta_{ij}\frac{\partial u_l}{\partial x_l}\right)\right]=\frac{\partial}{\partial x_j}\left(\mu\frac{\partial u}{\partial x_j}\right)+\frac{\partial}{\partial x_j}\left(\mu\frac{\partial u_j}{\partial x}\right)-0$$

$$=\frac{\partial}{\partial x}\left(\mu\frac{\partial u}{\partial x}\right)+\frac{\partial}{\partial y}\left(\mu\frac{\partial u}{\partial y}\right)+\frac{\partial}{\partial z}\left(\mu\frac{\partial u}{\partial z}\right)+\frac{\partial}{\partial x}\left(\mu\frac{\partial u}{\partial x}\right)+\frac{\partial}{\partial y}\left(\mu\frac{\partial v}{\partial x}\right)+\frac{\partial}{\partial z}\left(\mu\frac{\partial w}{\partial x}\right)$$

$$=\frac{\partial}{\partial z}\left(\mu\frac{\partial u}{\partial z}\right)$$

The turbulent diffusion term is

$$\frac{\partial}{\partial x_j}\left(-\rho\overline{u'u'_j}\right)=\frac{\partial}{\partial x}\left(-\rho\overline{u'u'}\right)+\frac{\partial}{\partial y}\left(-\rho\overline{u'v'}\right)+\frac{\partial}{\partial z}\left(-\rho\overline{u'w'}\right)$$

$$=\frac{\partial}{\partial x}\left(\mu_t\left(2\frac{\partial u}{\partial x}\right)\right)+\frac{\partial}{\partial y}\left(\mu_t\left(\frac{\partial u}{\partial y}+\frac{\partial v}{\partial x}\right)\right)+\frac{\partial}{\partial z}\left(\mu_t\left(\frac{\partial u}{\partial z}+\frac{\partial w}{\partial x}\right)\right)$$

$$=\frac{\partial}{\partial z}\left(\mu_t\frac{\partial u}{\partial z}\right)$$

For the equations of momentum balance in *y* and *z* direction, the simplification process is similar. Note that equation (2) does not involve acceleration of gravity, if gravitational force is considered, *z* direction momentum equation becomes

$$\frac{\partial p}{\partial z}=\rho g \tag{14}$$

2.2 ABL profile description

Atmospheric Boundary Layer (ABL), also known as Planetary Boundary Layer (PBL), is the lower part of the earth's atmosphere and its' behaviour is directly influenced by the contact with earth's surface. Generally, the ABL could be divided into 3 parts vertically[12], as illustrated in Figure 1. The lowest part is known as laminar bottom layer with a thickness equal to aerodynamic roughness length z_0, which is quiet small compare to the ABL height and could be neglected in most cases, that is $z \approx z+z_0$. For wind power engineering, typical value of roughness length is shown in Table 1[13]. In CFD model, the influence of this layer to upper wind flow is represented with wall functions instead of explicitly treated. Above z_0 is Prandtl or Surface layer where turbulence is fully developed, its vertical extent may vary from 20 to 100 meter, depending on the thermal stratifications of the air. Above the Prandtl layer is so called Ekman layer, which may reach a height exceeding 1000 m, depending on the stability of the air, Coriolis parameter and roughness height of the ground surface[13]. Above Ekman layer is free atmosphere, where the wind is approximately Geostrophic, the influence of ground surface roughness disappeared and flow turbulence almost vanished.

Table 1 Typical Surface Roughness Lengths

Type of terrain	Roughness length z_0
Cities, forests	0.7
Suburbs, wooded countryside	0.3
Villages, countryside with trees and hedges	0.1
Open farmland, few trees and buildings	0.03
Flat grassy plains	0.01
Flat desert, rough sea	0.001

The scales of turbulence in ABL is greatly depended on the thermal stratification, during the daytime with good solar radiation, temperature of ground surface is higher than air's, surface heating drives large thermal motions, that steadily intensify vertical momentum transport and increase the boundary's height, sometimes reach to 3000 m in late afternoon. This kind of stratification is said to be unstable. During night time, the temperature of ground surface may be lower than surrounding air, cooling of the ground surface results in suppression of turbulence scales and the boundary layer height may decrease to even 100 m. The stratification is then stable. If the effect of ground surface cooling or heating is relatively weak, often in late afternoon and during strong winds, turbulence is mainly generated by shear stress duo to velocity gradients and viscosity, the influence of temperature distribution could be neglected, this situation is named neutral stratification.
In the present work we consider a simplified ABL without division and in a neutral stratification. When it flows over a flat terrain, the horizontal mean velocity increase vertically with decreased increasing rate, and the turbulent shear stress decrease vertically. If only lower part of the ABL is considered, turbulent shear stress could be treated as constant and equal to wall shear stress. In this case, a constant shear stress should be defined at top boundary in CFD simulation. If all ABL height is in consideration, shear stress ought to be a variant along height and vanish at the top of ABL.

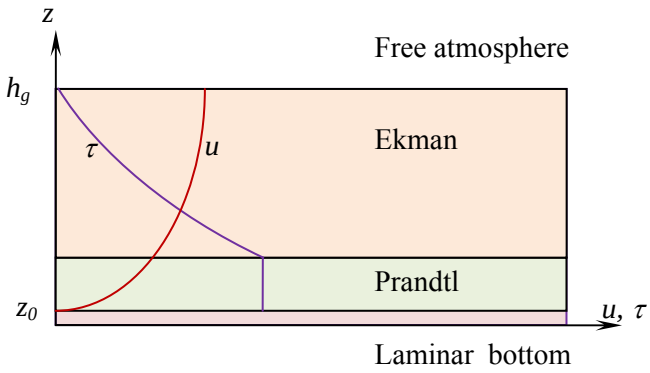

Figure 1 Subdivision of the Atmospheric Boundary, with conceptual illustration of vertical distribution of horizontal velocity and shear stress within the boundary layer

o Wind profile with constant shear stress

The following wind profile of horizontal velocity, turbulent kinetic energy and dissipation rate of kinetic energy for atmospheric boundary layer flows are widely adopted:

$$u = \frac{u^*}{\kappa} \ln\left(\frac{z}{z_0}\right) \tag{15}$$

$$k = \frac{u^{*2}}{\sqrt{C_\mu}} \tag{16}$$

$$\varepsilon = \frac{u^{*3}}{\kappa z} \tag{17}$$

Where u^* is abbreviation of u^*_{ABL}, Atmospheric Boundary Layer friction velocity, here assume it is equal to laminar bottom layer friction velocity $u_{\tau 0} = \sqrt{\frac{\tau_w}{\rho}} = \sqrt{\frac{\mu}{\rho}\frac{\partial u}{\partial z}\Big|_{z=0}} = \sqrt{\nu \frac{\partial u}{\partial z}\Big|_{z=0}}$, τ_w is the ground surface shear stress, ρ is density of air, μ and ν are dynamic and kinetic viscosities, respectively, and C_μ is a empirically model constant, for most industrial simulation, C_μ=0.09, but for wind flow simulation, a common choice is [14] C_μ =0.03. Richard and Hoxey[11] indicated that the set of equations (11~13) is accord with transport equation of turbulence kinetic energy (8), and they satisfy equation (9) under the following condition

$$\sigma_\varepsilon \left(C_{2\varepsilon} - C_{1\varepsilon}\right)\sqrt{C_\mu} = \kappa^2 \tag{18}$$

If the flow field is described as with equation (15~17), wall shear stress should be deduced as (here it is the shear stress at the centre of wall adjacent cell)

$$\frac{\partial u}{\partial z}\Big|_{z=z_p} = \frac{u^*}{\kappa z_p} = \frac{u_p}{z_p \ln\left(z_p / z_0\right)} \tag{19}$$

$$\mu_t = \rho C_\mu \frac{k^2}{\varepsilon} = \rho \kappa u^* z_p = \rho \kappa C_\mu^{\frac{1}{4}} k^{\frac{1}{2}} z_p \tag{20}$$

$$\tau_w = \mu_t \frac{\partial u}{\partial z}\Big|_{z=z_p} = \frac{\rho \kappa C_\mu^{\frac{1}{4}} k^{\frac{1}{2}} u_p}{\ln\left(z_p / z_0\right)} \tag{21}$$

Where subscript p denotes centre point of wall adjacent cell and z_p is the distance from p to wall surface. Note that equation (11~13) are based on the assumption that the turbulence kinetic energy, as well as the shear stress is constant along height, that is

$$\tau(z) = \mu_e \frac{\partial u}{\partial z} = \mu_t \frac{\partial u}{\partial z} = \rho C_\mu \frac{k^2}{\varepsilon}\frac{u^*}{\kappa \cdot z} = \rho \cdot u^{*2} = \tau_w \tag{22}$$

Where $\mu_e = \mu + \mu_t \approx \mu_t$ because $\mu_t >> \mu$ in fully developed high Reynolds number turbulent flow.
With above mentioned wind profile, momentum equation becomes

$$\frac{\partial p}{\partial x} = \frac{\partial}{\partial z}\left(\mu_t \frac{\partial u}{\partial z}\right) = \frac{\partial \tau}{\partial z} = 0 \tag{23}$$

As illustrate in Figure 1, a constant shear stress is reasonable if only lower part of the ABL is considered. If all ABL height is in consideration, a decreasing or piecewise decreasing function $k = f(z)$ should be adopted. In fact, a constant turbulence kinetic energy k and shear stress τ is deduced base on the assumption that the turbulent viscosity (or eddy viscosity) is proportional to height z [15]:

$$\mu_t = \rho C_\mu \frac{k^2}{\varepsilon} = \rho \kappa u^* z \tag{24}$$

The top of the atmospheric boundary layer is defined as turbulence equal to zero, that is, the turbulence at both bottom and top of the ABL almost vanish, the above equation could only be adopted for lower part of the ABL. Otherwise, along all height of ABL, the function of turbulent viscosity $\mu_t = f(z)$ should increase from zero at ground first, and then decrease to zero at top of the ABL.

- **Wind profile with decreased shear stress**

In present work, we still adopted equation (15), (17), but the turbulence kinetic energy profile is modified as:

$$k = \frac{u^{*2}}{\sqrt{C_\mu}}\left(1-\frac{z}{h_g}\right)^2 \tag{25}$$

Where h_g is Geostrophic plane elevation, or height of atmospheric boundary layer[13],

$$h_g = \frac{u^*}{6f} \tag{26}$$

f is Coriolis parameter, defined as

$$f = 2\Omega\sin(|\lambda|) \tag{27}$$

Where Ω is angular velocity of earth's rotation, Ω=7.2722×10^{-5} rad. λ is latitude of the position. If we take latitude as 55.5°, then f =1.1986×10^{-4}.

Here is an example. When aerodynamic roughness length z_0=0.03 m, wind speed is 8.5m/s at height of 10 m, we can get boundary's friction velocity $u^* = 0.5853$ m/s, turbulence kinetic energy at ground level is $k_0 = \frac{u^{*2}}{\sqrt{C_\mu}}$=2, and the height of boundary is h_g =813.8 m. Take air density as 1.225 kg/m3, the wall shear stress is $\tau_w = \rho \cdot u^{*2}$ =0.4196 N/m^2, and the wind velocity at the top of ABL is 23.35 m/s.

Combine equation (7), (17) and (25) we can get turbulence viscosity along height as

$$\mu_t = \rho C_\mu \frac{k^2}{\varepsilon} = \rho C_\mu \frac{\left(\frac{u^{*4}}{C_\mu}\right)\left(1-\frac{z}{h_g}\right)^4}{\left(\frac{u^{*3}}{\kappa z}\right)} = \rho\kappa u^* z\left(1-\frac{z}{h_g}\right)^4 \tag{28}$$

It will increase firstly from zero, get maximum at height of $h_g/5$, then decrease to zero at h_g.

Under the condition of decreased turbulence kinetic energy k (equation 17), shear stress and friction velocity are variants along altitude and reach to zero at the top of ABL:

$$\tau(z) = \mu_t \frac{\partial u}{\partial z} = \rho u^{*2}\left(1-\frac{z}{h_g}\right)^4 \tag{29}$$

$$u_\tau = \sqrt{\frac{\tau}{\rho}} = u^*\left(1-\frac{z}{h_g}\right)^2 \tag{30}$$

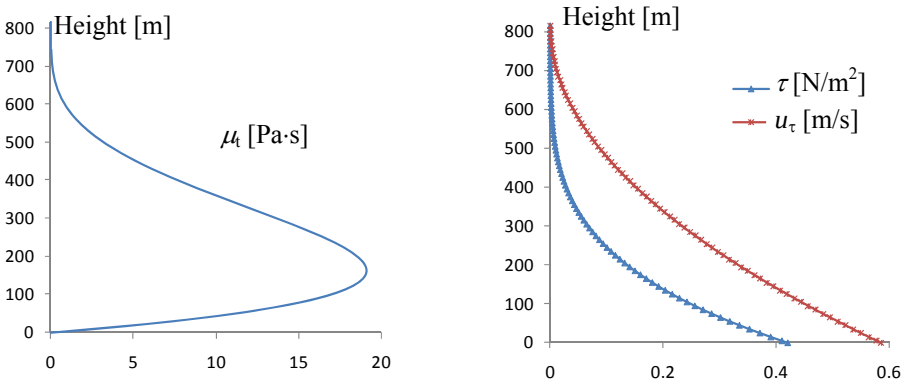

Figure 2 An example of turbulence viscosity, shear stress and friction velocity along altitude in the ABL according to equation 28, 29 and 30.

The set of wind profile equation (15), (25) and (17) doesn't match the transport equations of turbulence kinetic energy k and dissipation rate ε as described in standard k-ε model, that means with this wind profile as inlet and accordingly top and ground boundary conditions, the flow will not be homogenous over a flat terrain, pressure field is not uniform, but the CFD simulation could show that, with appropriate boundary conditions and wall treatment, speed up of velocity along stream direction could be within a limitation of 5% flowing over 8km length. The prominent difference between constant and variational shear stress wind profile is that, in the above mentioned variational shear stress condition, there is no driving force at the top of ABL, but in the constant shear stress condition, the ABL wind flow is drove by top boundary shear stress and restricted by ground friction (roughness). Neither of those two sets of wind profile are perfect, one could chose one according to the height of ABL interested.

2.3 Near wall treatment

For CFD simulation of turbulent wind flow based on RANS equation, the final flow field mostly depends on turbulence models and boundary conditions, especially ground wall treatment and other rational boundary settings. The ground surface, such as soil, vegetation, sand and stones, sometime even water surface, is impossible to be described directly with fine meshes in CFD simulation, their effect to wind flow must be represented with near wall treatment functions.

In Fluent 6.3, the standard wall functions are based on the proposal of Launder and Spalding (the Numerical Computation of Turbulent Flows. Computer Methods in Applied Mechanics and Engineering, 3:269-289, 1974.) And have been most widely used for industrial flows (Fluent 6.3 help reference[10]). Law-of-the-Wall for mean velocity modified for roughness has the form

$$\frac{u_P u^*}{\tau_w / \rho} = \frac{1}{\kappa} \ln\left(\frac{E u^* z_P}{\nu}\right) - \Delta B \tag{31}$$

Where suffix P means the centre of wall adjacent cell, $u^* = C_\mu^{1/4} k_P^{1/2}$ is friction velocity, k_P is turbulent kinetic energy, τ_w is shear stress, $\tau_w = \rho u_{\tau 0}^2$, $u_{\tau 0}$ is ground surface friction velocity, which is assumed equal to the ABL friction velocity u^*. E is an empirical constant and its value is 9.793. ν is kinetic viscosity. ΔB depends on the type and size of the roughness and has been found to be well-correlated with

the non-dimensional roughness height $Ks^+ = \frac{Ks \cdot u^*}{\nu}$. For fully rough turbulent flow, namely $Ks^+ > 90$, generally it is the condition of ABL flow, ΔB is

$$\Delta B = \frac{1}{\kappa}\ln\left(1 + Cs \cdot Ks^+\right) \tag{32}$$

Where Cs is roughness constant, for fully rough turbulent flow with $Cs \in (0.5,1.0)$, $Cs \cdot Ks^+ >> 1$, we have[10]

$$\Delta B \approx \frac{1}{\kappa}\ln\left(Cs \cdot Ks^+\right) = \frac{1}{\kappa}\ln\left(\frac{Cs \cdot Ks \cdot u^*}{\nu}\right) \tag{33}$$

With the assumption of $u_{\tau 0} = u^*$, combining Equation (31) and (32), yields:

$$\frac{u_P}{u^*} = \frac{1}{\kappa}\ln\left(\frac{Ez_P}{Cs \cdot Ks}\right) \tag{34}$$

The wind velocity profile is described with $\frac{u_P}{u^*} = \frac{1}{\kappa}\ln\left(\frac{z_P}{z_0}\right)$, equation (34) must be equivalent with wind velocity profile, that is

$$Ks = \frac{E \cdot z_0}{Cs} \tag{35}$$

The above equation indicates the difference and relationship between sand-grain roughness height and wind flow aerodynamic roughness length. The default value of roughness constant is Cs=0.5, correspond to uniform and-grain roughness, and for the most uneven roughness, Cs could be set to 1.0. Take the default value of Cs, if roughness length is 0.3 m, corresponding roughness height will be 6.0 m, with the restriction that the centre of wall adjacent cell should be higher than roughness height, the wall adjacent cell should be higher than 12 m, this is quite coarse mesh and always unacceptable. As indicated by D.M Hargreaves etc. [3] and Bert Blocken etc. [5] , the problem of streamwise gradients over flat terrain encountered by some previous simulation with commercial CFD software is firstly caused by setting roughness height as aerodynamic roughness length.
From equation (34) we can get the wall shear stress in standard wall functions

$$\tau_w = \frac{\rho \kappa C_\mu^{\frac{1}{4}} k_p^{\frac{1}{2}} u_p}{\ln\left(\frac{Ez_P}{Cs \cdot Ks}\right)} \tag{36}$$

Richard and Hoxey's method adopted roughness length and logarithmic profile directly, in their method the wall shear stress is described as

$$\tau_w = \frac{\rho \kappa C_\mu^{\frac{1}{4}} k_p^{\frac{1}{2}} u_p}{\ln\left(\frac{z_P}{z_0}\right)} \tag{37}$$

Equation (36) and (37) are equivalent if roughness height *Ks* is set according to equation (35) in Fluent. As indicated before, this will limit wall adjacent cell's fineness. Bert Blocken [5] considered another choice that directly set wall shear

stress with constant $\tau_w = \rho u^{*2}$ as a boundary condition, that will force $u_{\tau 0} = u^*$. This method could be adopted as a substitute of unacceptable large roughness height, but it only works for flat terrain with uniform roughness, because wall shear stress will change over complex terrain.

The production rate of turbulence kinetic energy at the centre of wall adjacent cell could be written referencing shear stress, $P_k = \mu_t \left(\frac{\partial u}{\partial z} \right)^2 = \tau_w \frac{\partial u}{\partial z}$, in standard wall functions with logarithmic description of velocity, $\frac{\partial u}{\partial z} = \frac{u^*}{\kappa} \cdot \frac{1}{z_p}$, here $u^* = \frac{\kappa u_p}{\ln\left(\frac{E z_P}{Cs \cdot Ks} \right)}$ and $u_p = \frac{\tau_w \cdot \ln\left(\frac{E z_P}{Cs \cdot Ks} \right)}{\rho \kappa C_\mu^{\frac{1}{4}} k_p^{\frac{1}{2}}}$ according to equation (34) and (36), respectively, then

$$P_k = \frac{\tau_w^2}{\rho \kappa C_\mu^{\frac{1}{4}} k^{\frac{1}{2}} z_p} \tag{38}$$

This is how the production rate of turbulence kinetic energy is computed for wall adjacent cells in so called standard wall functions[10]. In Richard and Hoxey's method which could produce homogenous wind flow over flat terrain, the production rate of turbulence kinetic energy at centre of wall adjacent cell is the same expression, the difference is that Fluent take the centre value of P_k as cell value, here we named it as uniform P_k, Richard and Hoxey evaluate the mean production rate with a integral

$$P_k = \int_{z_0}^{2z_p} \frac{P_k}{2z_p} dz = \frac{\tau_w^2}{\rho \kappa C_\mu^{\frac{1}{4}} k^{\frac{1}{2}} 2z_p} \ln\left(\frac{2z_p}{z_0} \right) \tag{39}$$

Which we named as integral P_k. The integral method is reasonable. If we adopt standard wall functions and want an effect of integral mean value, the centre height of wall adjacent cell should be set with the following relationship

$$\frac{1}{z_p} = \frac{1}{2z_p} \ln\left(\frac{2z_p}{z_0} \right) \Rightarrow \ln\left(\frac{2z_p}{z_0} \right) = 2 \Rightarrow z_p = 3.69 z_0 \tag{40}$$

If z_0 =0.03m, the centre of first cell should be 0.1107m to produce appropriate kinetic energy. Otherwise if z_p >3.69 z_0, $\frac{1}{z_p} < \frac{1}{2z_p} \ln\left(\frac{2z_p}{z_0} \right)$, production rate of turbulence kinetic energy in standard wall functions is smaller than it ought to be.

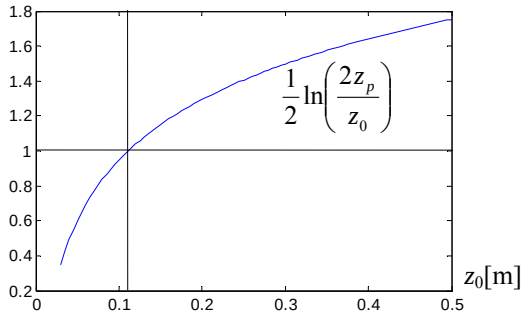

Figure 3 The value of integral P_k over uniform P_k when z_0=0.03

2.4 Closure

1) Mathematically, the wind profile equation (15~17) agree with transport equation of k and ε, along with corresponding wall treatment and a constant shear stress boundary condition at the top, it is proven that the modified k-ε two-equation RANS CFD model could produce a homogenous flow over a flat terrain.
2) The standard k-ε two-equation model in Fluent, especially the near wall treatment of roughness, shear stress and production rate of kinetic energy, does not satisfy homogenous requirement. A modification of turbulence model is needed to implement homogenous flow in Fluent. And most important is a shear stress boundary at top boundary resulted from constant shear stress assumption.
3) Logarithmic wind velocity is only an approximate description of real ABL flow, homogenous flow over flat terrain is a good tool to examine CFD model but is not the ultimate final. Constant shear stress assumption deviate from actual situation of ABL flow, decreasing shear stress is more appropriate. Descending shear stress does not fully satisfy default transport equation of k and ε in Fluent then wind flow over flat terrain could not be homogenous.
4) The standard wall functions are based on pipe flow experiments with sand-grain roughness which is very different from ground roughness, a wall roughness modification is always necessary to simulate wind flow with Fluent.

3 Simulation of a flat terrain

In order to investigate the consistence of ABL profile of velocity and turbulence with standard k-ε 2-equation model along with standard wall functions of Fluent, wind flows over a flat terrain is simulated.The wind profiles adopted in the simulations are defined with equation (15), (17) and (25). To deal with the roughness height problem in Fluent, a new wall roughness function is implemented with User Defined Functions in Fluent.

3.1 Simulation case description

1. **Meshing schemes of the simulation domain**

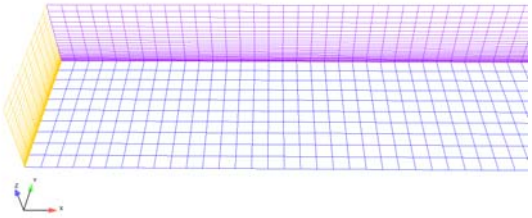

Figure 4. Mesh of part of the simulation domain

Computational domain is: Length (x) =10,000m, Width (y) =1,000m, Height (z) =500m. For length and width direction, the interval size of mesh is 100m with uniform interval size meshing scheme. For altitude direction, the meshing scheme is successive ratio (geometric progression), that is, the ratio of any two succeeding interval length is constant: $R = \Delta z_{i+1} / \Delta z_i$. If interval count is N, there are totally N+1 nodes, the length of the line is $L_z = \sum_{i=0}^{N} \Delta z_i = \sum_{i=0}^{N} \Delta z_1 R^i = \Delta z_1 \frac{1-R^N}{1-R}$, the first interval size is

$$\Delta z_1 = L_z \frac{1-R}{1-R^N} \tag{41}$$

Here the successive cell height ratio is R=10/9, L_z=500m and N=40, height of the first cell (wall adjacent cell) is 0.8335m, the central point is $z_P = 0.4168$ m. Total cell number is 100×10×40.

The above mentioned is a coarse mesh, which is used to compare with the finer mesh. The refinement scheme is illustrated in Figure 5, where only the wall adjacent cells are refined through dividing each cell into four identical cells. For present work of flat terrain simulation, the finer mesh is default one to be adopted, where the centre of the first cell is z_P=0.208 m, that is a half of coarse mesh's.

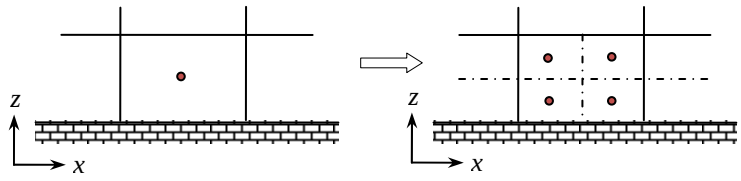

Figure 5 Refinement of wall adjacent cells

2. CFD models

The simulation apply second order pressure interpolation based solver, pressure-velocity coupling is carried out with SIMPLE algorithm, discretization schemes for momentum and TKE, TDR are all second order upwind algorithm.

Standard k - ε 2-equation turbulence model along with standard wall function are applied with constants shown as Table 2:

Table 2 Default and modified model constants

constants	C_μ	$C_{\varepsilon 1}$	$C_{\varepsilon 2}$	σ_k	σ_ε
default	0.09	1.44	1.92	1.0	1.3
modified	0.03	1.21	1.92	1.0	1.3

The above set of modified constants for standard k - ε model satisfy equation (18): $\kappa^2 = (C_{\varepsilon 2} - C_{\varepsilon 1})\sigma_\varepsilon \sqrt{C_\mu}$, where σ_ε is turbulent Prandtl number for ε , Von Karman constant is κ =0.4.

3. Wind profile and boundary conditions

Vertical profiles for the mean wind velocity u , turbulent kinetic energy k and turbulent dissipation rate ε in the atmospheric boundary layer are set according to equation (15), (17) and (25), with κ =0.4 and modified constant C_μ=0.03. Parameters adopted in the simulation are shown in Table 3.

Table 3 Parameters of the Wind flow

Parameter	u^*[m/s]	z_0[m]	h_g[m]	ρ[kg/m^3]	μ[kg/(m·s)]
Value	0.6541	0.03	909.56	1.25	1.7894×10^{-5}

According to equation (28) and the wind flow parameters, the maximum value of turbulent viscosity is

$$\mu_{t\max} = \rho\kappa u^* \frac{h_g}{5}\left(\frac{4}{5}\right)^4 = 23.88 \quad [\text{kg/(m·s)}]$$

From which we can estimate the turbulent (eddy) viscosity ratio as $\mu_{t\max}/\mu = 1.335\times10^6$. This value is larger than common industrial internal flow's. In Fluent the default limit for turbulent viscosity ratio is 1×10^5, it is necessary to magnify the limit to 2×10^7 or even larger for wind flow simulation.

The flow is along x direction, outflow boundary condition is imposed on the end plane of the domain, both sides are symmetry, and the top plane is defined as velocity inlet boundary where the velocity, turbulence kinetic energy and dissipation rate are calculated with inlet wind profile equations. The bottom of the domain is no-slip ground wall.

The boundary conditions for inlet, top and ground wall are implemented with User-Defined Functions in Fluent. Other kind of boundary conditions for top plane are tried, such as moving wall at same speed with adjacent air flow, symmetry and outflow with zero mass flow rate, but the results cannot prove they are better choice.

3.2 Problem analysis

For the first simulation, roughness height *Ks* is set equal to roughness length z_0, which is a wrong setting because they are very different. Fine mesh and standard wall functions are adopted along with default model constants.

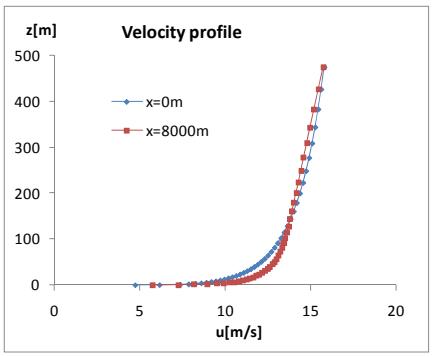

(*a*)

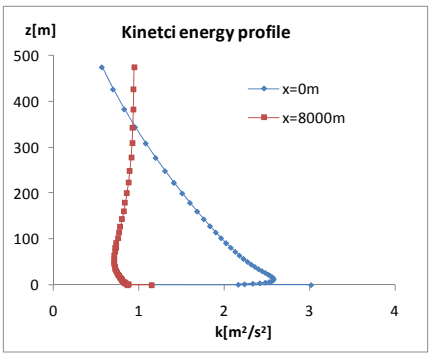

(*b*)

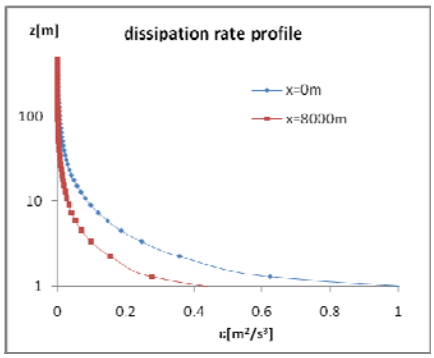

(*c*)

Figure 6 Simulation results from case with Ks=0.03, standard wall function and default model constants. Wind profiles of (a) wind velocity. (b) Kinetic energy. (c) Kinetic energy dissipation rate.

The above figure shows the results from the simulation, comparison of wind profiles at inlet of the flat terrain domain and along a vertical line located at 8000 m downstream. The wind flow is far from homogenous. From the velocity profiles we can estimate that ①the turbulence transport in the CFD model is stronger than what necessary to get homogenous velocity profile, ②the wall functions modified for roughness provide relatively weaker influence to the lower part of the wind flow. For the first estimation, we may assume that a smaller model constant C_μ should be appropriate, and we can find that the modified C_μ, which is calculated from equation (16) according to site measurements of velocity profile and turbulence kinetic energy, is smaller than default value.The second one could be a conclusion because according to equation (35), roughness height should be almost 20 times of the roughness length. From the speed up of turbulence kinetic energy we can estimate that the production of kinetic energy in near wall zone is smaller than what described by the inlet wind profiles. This could be answered by Figure 3 that with a larger z_p, uniform P_k is smaller than integral P_k, still with standard wall functions modified for roughness height, z_p's approaching to $3.69z_0$ should improve the flow-wise consistency of turbulence kinetic energy.

3.3 User-defined wall functions

The standard wall functions modified for roughness could be adopted with amplifying Roughness Height *Ks* as $\frac{E \cdot z_0}{Cs}$, where $E = 9.793$ and C_S=0.5 as default. But according to Fluent user's guide, "it is not physically meaningful to have

a mesh size such that the wall-adjacent cell is smaller than the roughness height. For best results, make sure that the distance from the wall to the centre of the wall-adjacent cell is greater than Ks"[10]. This requirement will result in unacceptable coarse mesh with a large roughness length z_0.

A user defined wall function for near-wall treatment is designed to solve this problem adopting roughness length instead of roughness height. Working with $k-\varepsilon$ 2-equation turbulence model, the user-defined wall function is designed according to ABL wind velocity profile, $\frac{u}{u^*}=\frac{1}{\kappa}\ln\left(\frac{z}{z_0}\right)$, assuming $u^*=u_{\tau 0}$:

Laminar bottom layer:

$$u^+=z^+ \tag{42}$$

Fully turbulent region (Log law region):

$$u^+=\frac{1}{\kappa}\ln\left(\frac{z_p}{z_0}\right)=\frac{1}{\kappa}\ln\left(\frac{u_{\tau 0}z_p}{\nu}\frac{\nu}{z_0u_{\tau 0}}\right)=\frac{1}{\kappa}\ln\left(z^+\cdot\frac{\nu}{z_0u_{\tau 0}}\right)=\frac{1}{\kappa}\ln\left(\frac{z^+}{Z_0^+}\right) \tag{43}$$

Where $u^+=\frac{u_p}{u_\tau}$ is dimensionless wall tangential velocity. $z^+=\frac{u_\tau z_p}{\nu}$, where $u_{\tau 0}=\sqrt{\frac{\tau_w}{\rho}}$ is the friction velocity, z_p is the distance from the wall adjacent cell centre to wall surface, $\nu=\frac{\mu}{\rho}$ is kinetic viscosity of air. $Z_0^+=\frac{z_0u_{\tau 0}}{\nu}$ is dimensionless roughness length of the ground. With the user defined wall functions, Roughness height is not necessary, roughness length z_0 is defined in wall function directly, but as a required input parameter, it is always set to the same value of roughness length in the following simulation cases.

In fluent, laminar bottom boundary layer is defined as $z^*=\frac{C_\mu^{\frac{1}{4}}k_p^{\frac{1}{2}}z_p}{\nu}\le 11.225$, logarithmic law will be adopted if $z^*>11.225$. z^* and z^+ are approximately equal in equilibrium turbulent boundary layers.

3.4 Results from different model settings

Simulations of wind flow over flat terrain with different model settings are carried out, the basic model is as described in section 3.1, and adjustable settings are ground wall and top boundary conditions such as amplified roughness height, constant wall shear stress ($\tau_w=\rho u^{*2}$) with roughness height same to roughness length, user defined wall function with roughness height same to roughness length, symmetry top boundary, moving wall top boundary, and the default is velocity inlet top boundary condition. Some typical results are reported as follow. It should be noted that constant wall shear stress ground wall boundary condition can achieve very close result get from amplified roughness height, but that is only suitable for steady-state flat terrain wind flow, for wind flow over complex terrain, wall shear stress could not be constant, the results from constant wall shear stress setting are not reported.

Case 1. Roughness height set as equal to roughness length (*Ks*=0.03), Standard wall functions, **modified model constants**, finer mesh (Figure 7).

Here we assume inlet wind profiles are good description of neutral wind flow over flat terrain. Compare with Figure 6, the only difference is model constant, we can conclude that the modified model constant could improve simulations result.

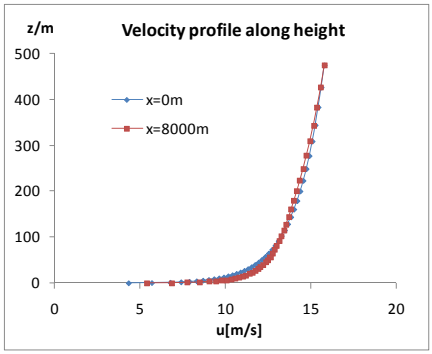

(*a*)

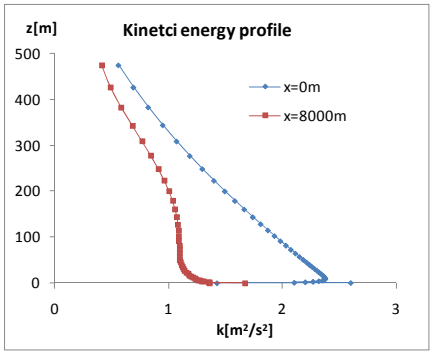

(*b*)

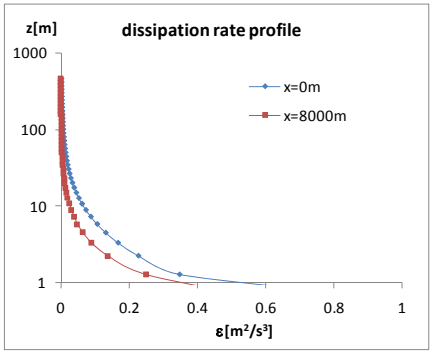

(*c*)

Figure 7 Simulation results from case with Ks=0.03, standard wall function and ***Modified model constants****.(a) profile of wind velocity.(b) profile of kinetic energy.(c)profile of kinetic energy dissipation rate.*

Case 2. Roughness height set as 20 times roughness length (***Ks*=0.6**), Standard wall functions, modified model constants, finer mesh (*Figure 8*).

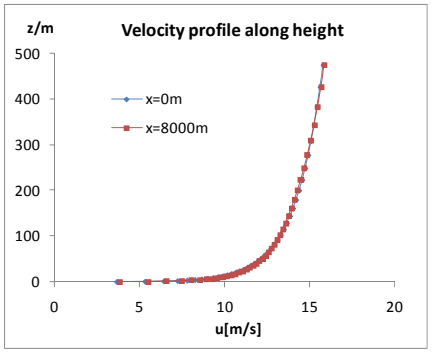

(*a*)

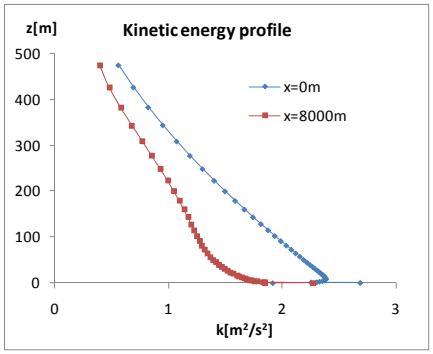

(*b*)

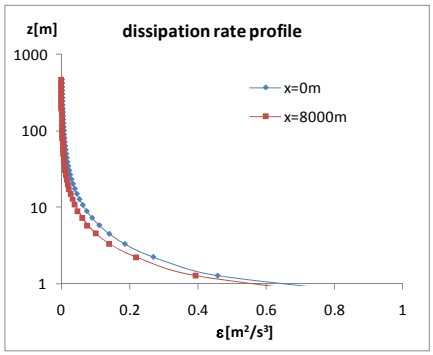

(*c*)

Figure 8 Profiles of velocity (a), turbulence kinetic energy (b) and dissipation rate (c) at inlet and 8000 m downstream. ***Ks=20·z₀.***

This case is an improvement from case 1, with $Ks=20 \cdot z_0$, the roughness height in the CFD model is consistent with aerodynamic roughness length adopted in the inlet wind profile description. Amplified roughness height could produce wind velocity profile almost without flow-wise gradients (*Figure 8* (*a*)).
It should be noted that in this case, Ks=0.6m is higher than wall adjacent cell centre z_p=0.208m, according to Fluent user's guide, a higher roughness height is unreasonable. The code can implement the simulation and produce above mentioned result, but the manipulation process is unknown. As recommended by the user's guide, a roughness height larger than z_p should be avoided.

Case 3. User-defined wall functions, Roughness Height set as Roughness Length, Ks=0.03, modified model constants, finer mesh (Figure 9).
This is another method to express the influence of ground roughness instead of applying an amplified roughness height. The user defined wall functions are designed and implemented by the authors. Compare Figure 9 with *Figure 8* we can see that the user defined wall functions could achieve even better results. Furthermore,

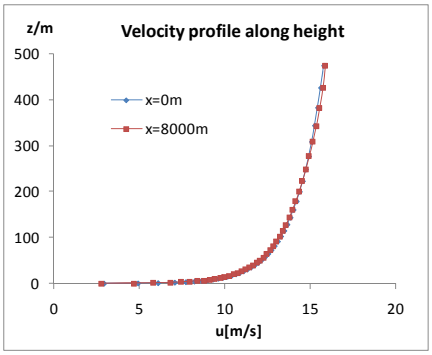

(*a*)

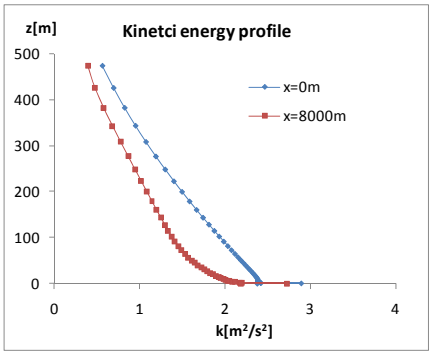

(*b*)

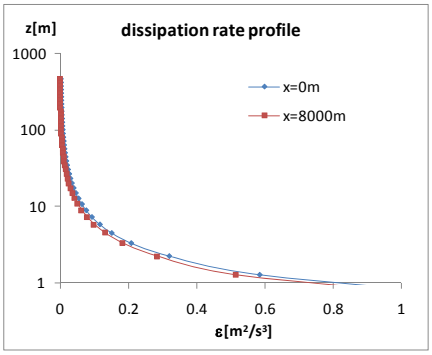

(*c*)

Figure 9 Simulation results from case with Ks=0.03, ***user defined wall functions*** *and Modified model constants.(a) profile of wind velocity.(b) profile of kinetic energy.(c)profile of kinetic energy dissipation rate.*

Case 4. Roughness height set as 20 times roughness length (Ks=0.6), Standard wall functions, modified model constants, **coarse** mesh.
This case is not an improvement but to show influence of mesh fineness. The only difference of case 4 from case 2 is that case 4 applied a coarse mesh, z_p=0.417m, twice the length in case 2. Mesh along x and y directions are the same with case 2. The results show that a suitable fineness of vertical mesh is important to get a flow closer to homogenous one.

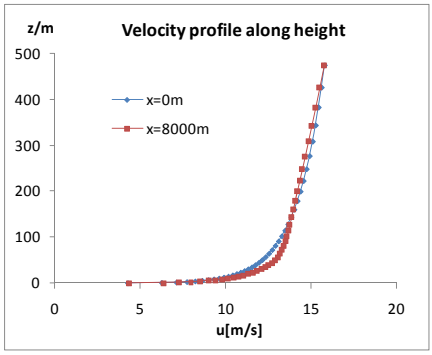

(*a*)

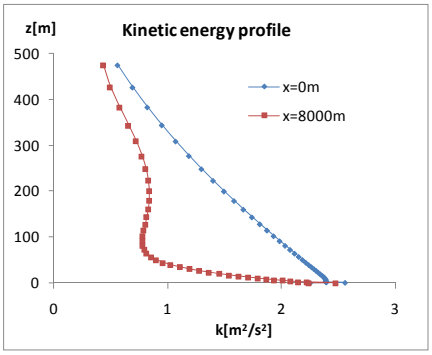

(*b*)

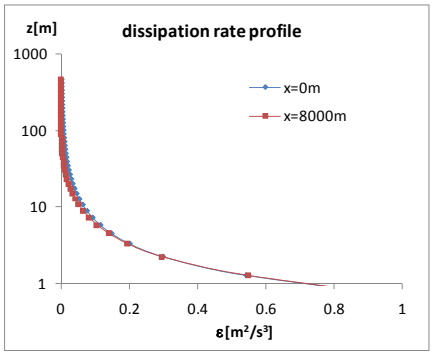

(*c*)

Figure 10 Simulation results from case with Ks=0.6, standard wall function, modified model constants and coarse mesh (z_p=0.417m).(a) profile of wind velocity.(b) profile of kinetic energy.(c)profile of kinetic energy dissipation rate.

3.5 Comparison and conclusion

To compare consistence of CFD model with inlet wind profile description, we define speed up as

$$\Delta M = \frac{M(x=8000,z)-M(x=0,z)}{M(x=0,z)} \tag{44}$$

Here M could be velocity, turbulence kinetic energy or dissipation rate of turbulence kinetic energy.

With user defined wall functions or amplified roughness height, finer mesh and modified model constants, the standard k-ε model can produce nearly homogenous mean wind velocity profile (Figure 11), most points of speed up are within a limit of 2%, the largest speed up from amplified roughness height fall into a range of 5%, and for user defined wall functions method, only 2 lowest points of speed up are slightly more than 5%.

At the aspect of turbulence kinetic energy and its' dissipation rate, the flow is far from homogenous with the present CFD model. The user defined wall functions method produce the best results, where the speed up of k is around 30 %(Figure 12), speed up of ε is increasing along height with modified model constants (Figure 13), under the height of 200 m, user defined wall functions method produce best result, even so the largest speed up is nearly 50%.

The EllipSys3D code could handle the homogenous problem perfectly [1]. Another well known homogenous wind flow CFD model is the one contrived by Richards and Hoxey, denoted as RH, and implemented using a version of PHOENICS (2005) which can be re-compiled[3, 11]. Furthermore, to get a homogenous wind flow with RH model, it is important to set a constant shear stress top boundary condition along with the modified ground wall functions, with assumptions of constant shear stress along altitude and ABL flow is driven by Geostrophic wind. For Fluent, it is not

possible to produce a sustained wind flow over flat terrain without complex modifications of viscous model. Until now we can see that with standard k-ε model, the results from user defined wall functions method is closest to sustained wind flow.

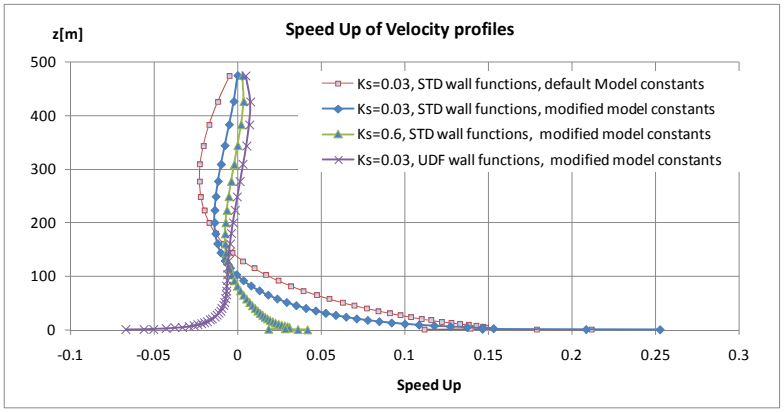

Figure 11 Comparison of speed up of mean velocity

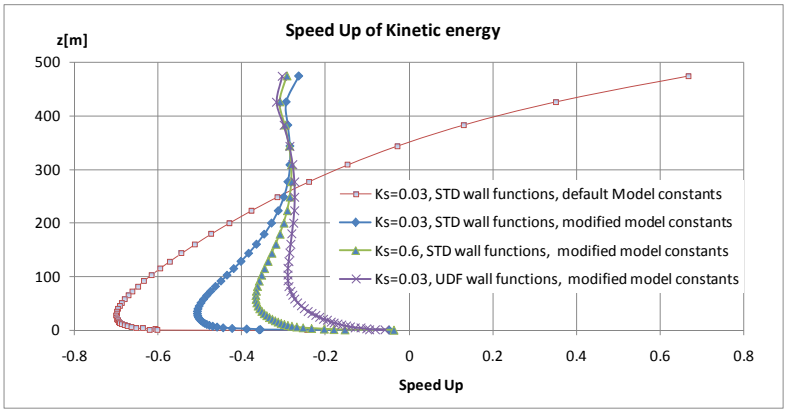

Figure 12 Comparison of speed up of kinetic energy

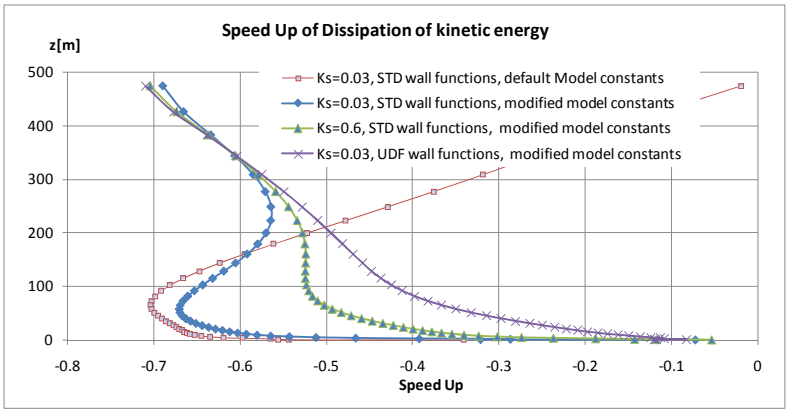

Figure 13 Comparison of speed up of dissipation of kinetic energy

3.6 Closure

The standard k-ε 2-equation model in Fluent along with corresponding near wall treatment functions are based on internal industrial flow and sand-grain wall roughness experiments. The wall functions modified for roughness, near wall production of turbulence kinetic energy and default viscous model constants are not suitable for the simulation of ABL flow. To obtain a flow field over flat terrain close to sustained wind flow, the following aspects are important

①Modification of model constants ABL flat terrain flow simulation should adopt a C_μ smaller than its' default value of 0.09, to mitigate the decay of turbulence kinetic energy along flow direction, diminish momentum transport in mean flow. 0.03 is used for present work, a smallest value of 0.013 is suggested by literatures. Other model constants should be changed according to C_μ.

②Ground roughness wall functions should be modified. The simplest way is still use standard wall functions but applies an amplified roughness height *Ks*, with a limitation that the wall adjacent cell centre should be higher than *Ks*, this limitation may result in coarse mesh. A better choice is to use a user defined wall function set adopting roughness length directly, this could achieve better flow pattern and get rid of the coarse mesh limitation.

③Fineness of mesh do play a role in the simulation. To get a suitable near wall production of turbulence kinetic energy, height of first cell (wall adjacent cell) centre should be close to $3.69 \cdot z_0$. A geometric increase scheme is recommended for the grid along altitude.

④Logarithmic mean velocity profile is widely adopted, constant turbulence kinetic energy profile is suitable for lower part of ABL flow, and for whole ABL flow, a decreasing distribution should be a better choice. Improvement of wind profile will basically benefit CFD simulation, that did not included in present study.

⑤According to Hargreaves and Wright[3], a homogenous wind flow must be driven by a shear stress at the top boundary. This conclusion is based on constant kinetic energy, uniform pressure field, as well as constant shear stress assumptions and it is not in accordance with neutral ABL flow description in all depth. With decreasing kinetic energy assumption, turbulence viscosity should vanish at the top of ABL, shear stress at top plane is weak and cannot be the main driven force for ABL flow. The driven force of the flow should include pressure gradients, which, until now, have not been considered in the CFD model study.

4 CFD Simulation of the Askervein Hill

The Askervein hill project was a field measurements study carried out during September- October 1982 and 1983, around Askervein (Figure 14), a 116m high hill on the west coast of the island of South Uist in the Outer Hebrides of Scotland[16]. The experimental data were made available in 1983 [17]and 1985[18] and from then on, become the best known, most extensive and most complete field measurements. Until now, fully replicate the measured wind flow with CFD simulation is still a big challenge. In this chapter, we will use the standard k-ε model, which was adjusted through flat terrain simulations, to undertake the simulation task of Askervein hill wind flow.

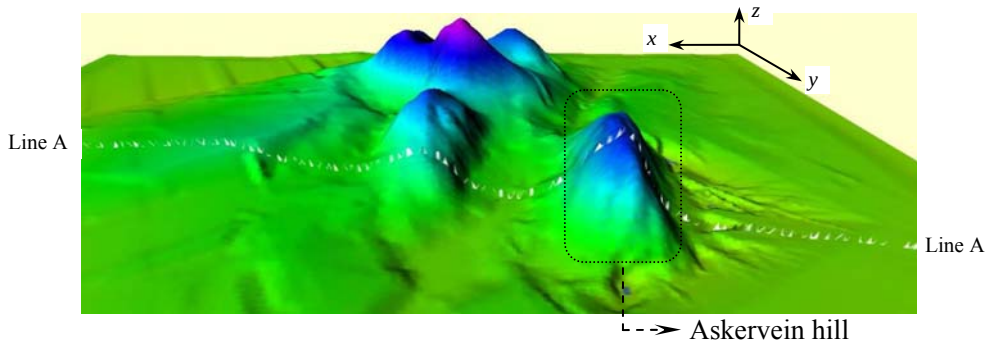

Figure 14 Perspective view of Askervein hill and surrounding ground and hills. The elevation scale is magnified 5 times with respect to the horizontal scale

4.1 Simulation domain and mesh scheme description

Figure 15 shows the ground range and a meshed side plane of the simulation domain. The ground map has been oriented so that the *x*-axis is aligned with the mean wind flow direction at the time of measurements (210°*N*). The horizontal range of considered ground is from (-2793, -3793) to (5895.1, 1769.7) in Cartesian coordinates with *z* direction represent altitude. So the simulation domain is 8688.1 m in length and 5562.7 m in width, with elevation of top plane at *z*=1500 m. Elevation of ground surface is variant from 0 to 160 m. Askervein hill locate at the top-left part of the ground map with its' highest point marked HT, coordinates are (23.275, 233.575, 123.79). The highest point is 116 m above surroundings. Askervein hill is relatively isolated from nearby bigger hills where a highest point's coordinates are (1024, -1442, 160). Upstream of Askervein hill there is a uniform and flat fetch extend about 4km to the coastline. 3km upstream, where the inlet plane of the simulation domain is located, there is a reference site (RS). During the measuring period, 50m high wind towers were sited at HT and RS. Calculated wind profiles based on the measurement from RS is used as inlet boundary condition. There is a line marked A-A and referenced as Line A in the domain, 10m above ground surface, some measuring instruments were located along this line. CFD simulation results are compared with measured data from line A and HT. The Field experimental data adopted in the CFD simulation for boundary conditions and results comparison is TU-03B (Table 4).

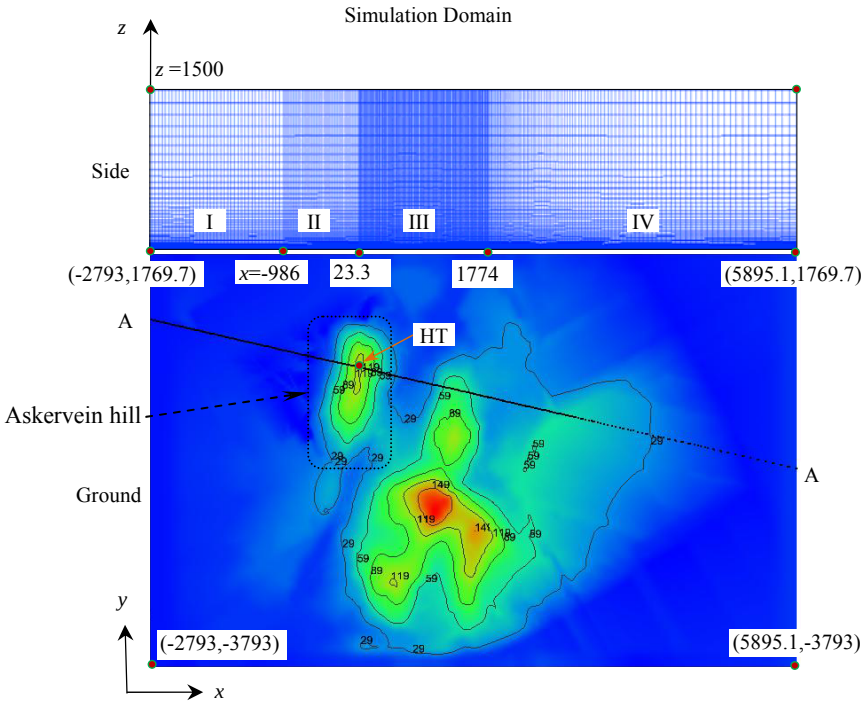

Figure 15.Ground map include elevation contours (m) *of the Askervein hill and nearby terrain used in CFD simulations, the upper part is a meshed vertical side plane of the simulation domain.*

The domain is divided into 4 zones along *x* direction marked I, II, III, IV, to adopt a finer mesh for the hill zone. In *x* direction, zone I, II, III are meshed with uniform interval size, Δx_I=46m, Δx_{II}=23m, Δx_{III}=11.5m, Zone IV is meshed applying Successive Ratio scheme with average Δx_{IV}=46m. For whole domain in y direction, cell length is uniform, Δy=46m.

The basic mesh scheme along height direction is Successive Ratio with wall adjacent cell height of 2.0 m, interval count of 50 and increasing ratio of 1.087. Then the wall adjacent cell layer is split into two layers, finally the vertical mesh interval count is 51 and bottom cell height is 1.0 m. Totally cell volume number is about 2 million.

4.2 CFD model and field measurements

The CFD model apply second order pressure interpolation based solver, pressure-velocity coupling is carried out with SIMPLE algorithm. Two kinds of discretization schemes for momentum and TKE, TDR are applied, one is second order upwind algorithm, and the other is QUICK algorithm.

Standard k - ε 2-equation turbulence model along with user defined wall functions are applied with constants shown as following:

$C_\mu = 0.03$, $C_{\varepsilon 1}$= 1.21 , $C_{\varepsilon 2}$= 1.92 , σ_k= 1.0 , σ_ε= 1.3

This set of constants is taken the same as model for flat terrain simulation. Assume the roughness height of the ground surface is a constant value of 0.03[16], the measured mean velocity data was fitted with a logarithmic expression and get a friction velocity u^*=0.6183 m/s, Inlet velocity profile (Figure 16) is:

$$u = \frac{u^*}{\kappa}\ln\left(\frac{z-2.998}{z_0}\right) \tag{45}$$

Where $u^* = 0.6183$ m/s, $\kappa = 0.4$ is von-Karman constant, $z_0 = 0.03$ m, 2.998 m is the ground height at inlet plane, it is constant along *y* direction.

$$k = \begin{cases} \dfrac{u^{*2}}{\sqrt{C_\mu}}\left(1-\dfrac{z-2.998}{Hg}\right)^2 & z < Hg + 2.998 \\ 0.0001 & z \geq Hg + 2.998 \end{cases} \tag{46}$$

$$\varepsilon = \frac{u^{*3}}{\kappa(z-2.998)} \tag{47}$$

Where Hg =859.77m is height of ABL flow. Note that in equation (46), kinetic energy will not be initialized with zero at height higher than ABL, because mean velocity gradient doesn't vanish, zero turbulence is not acceptable for this turbulent flow, so a relatively small value is used and in implementation, *k* change continuously along altitude. Some efforts were made to run the simulation with constant turbulence kinetic energy vertically at inlet, but it is difficult to get to convergence, especially with finer mesh, the iteration runs into divergence.

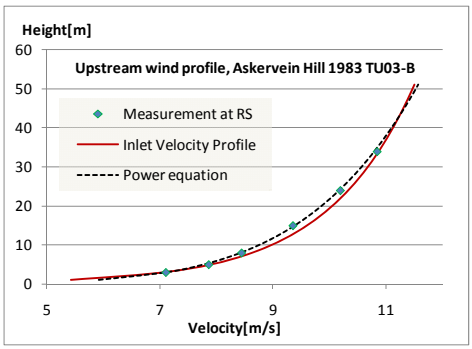

Figure 16 Mean wind velocity measurement from RS (Runs TU03-B) and corresponding logarithmic and power wind profile

Measurements of mean wind speed and mean fluctuating wind speed along line A are shown in Table 4, all those anemometers were mounted 10 meters high above ground surface. Measurements from vertically mounted anemometers at sites RS and HT are shown in Table 5. Both tables are taken from field measurement RUN No. TU03-B[18], which was taken on October 3rd, 1983, where the atmospheric boundary layer was nearly neutrally stratified. This is the most commonly used dataset.

Table 4. Measurements taken along line A at 10m above ground level. Runs No. TU03-B, AES vertical Gill UVW anemometer. Askervein 83 Project.

dist.HT [m]	direction [°]	Up wash [°]	Speed [ms^{-1}]	<u'> [ms^{-1}]	<v'> [ms^{-1}]	<w'> [ms^{-1}]
RS	207.3	2.5	8.6	1.223	0.704	0.413
-850	201.6	3.9	7.8	1.200	0.762	0.463
-500	192.9	2.8	6.7	1.350	0.683	0.475
-350	196.0	11.5	7.2	1.243	1.038	0.580
-200	200.6	16.0	10.5	1.115	1.126	0.565
-100	207.9	14.5	13.2	1.059	1.232	0.577
HT	203.4	2.7	16.2	1.100	1.034	0.577

100	206.5	-11.1	12.0	1.758	1.012	0.531
200	195.9	-13.0	5.6	2.560	1.502	0.881
400	188.1	-5.7	3.0	1.983	1.798	1.192

Table 5. Vertically measurements from RS and HT. Runs No. TU03-B, AES cup anemometer. Askervein 83 Project.

Height [m]	Speed(RS) [ms^{-1}]	<u'>(RS) [ms^{-1}]	Speed(HT) [ms^{-1}]	<u'>(HT) [ms^{-1}]
3	7.10	1.42	15.71	1.45
5	7.86	1.37	16.38	1.38
8	8.44	1.42	16.30	1.17
15	9.35	1.27	16.63	1.04
24	10.19	1.23	16.15	1.19
34	10.84	1.16	15.77	1.17

The measurements cannot be in fully accordance with inlet wind profiles applied in the CFD model, and we take mean velocity profile as the first important. Along line A which is 10m above ground, including the point at RS, measurements were implemented with AES vertical Gill UVW anemometers. Along RS and HT, excluding the 10 m high point, measurements were implemented with AES cup anemometers. The logarithmic profile of mean wind velocity is derived from vertically measurements from RS in Table 5, the expression does not cover measurements exactly. On the aspect of turbulence kinetic energy, equation (46) produces relatively larger value for inlet k. Re-evaluation of equation 46 with measurements of k in Table 4 will suggest a larger model constant C_μ

$$C_\mu = \frac{u^{*4}}{k^2}\left(1-\frac{10}{Hg}\right)^4 = 0.119$$

This value is even larger than the default 0.09. From the simulation experience of flat terrain we hold that C_μ should be smaller than default value. In present simulation we still use a C_μ=0.03, the simulation results show that this value is accepthable to produce reasonable relative turbulent kinetic energy k/u^2 in the flow field.

The dataset at RS is taken as reference of whole flow field. But note that there are different set of reference values at this site. The fundamental measurements are shown in Table 5, if continuous expression is needed, a better curve fitting of mean wind speed along line RS gives following equation (Figure 16)

$$u(z) = 5.927 z^{0.17} \tag{48}$$

And of course the logarithmic equation is an expression of the measurements at RS too. It is not the best curve for those measured points but we hold that the logarithmic expression include all measured wind information there.

The 10m height is most important and the AES vertical Gill UVW anemometer gives a mean speed of 8.6 m/s for RS. There were two other kind of anemometers mounted at that site, one is Tilted Gill UVW anemometer, the other is Sonic anemometer, both of them gave mean wind speed larger than 8.6 m/s. But because all other points along line A were measured with AES vertical Gill UVW anemometers, we take 8.6 m/s as a basic reference for measurements along line A. In contrast, equation (48) gives a value of 8.767 m/s for the point 10 m high at RS, and logarithmic expression gives a value of 8.979 m/s for the same point. The simulation adopted logarithmic profile as inlet, so we take 8.979 m/s as reference for normalization of simulation results along line A.

4.3 Results

In order to compare the mean wind velocity from CFD simulation with field measurements, we define the speed-up, as difference between local wind speed and undisturbed reference wind speed normalized with the reference wind speed:

$$\Delta S = \frac{U_{loc}(h) - U_{ref}(h)}{U_{ref}(h)} \tag{49}$$

Where h is local height above ground, U is velocity magnitude. For normalization of wind speed along line A or other points 10 m above ground, $U_{ref,m}$=8.6 ms^{-1} is taken as reference wind speed for measured data, $U_{ref,s}$=8.979 ms^{-1} is taken as reference wind speed for simulation results. For normalization of vertical wind speed, equation (48) is taken as continuous reference.

4.3.1 Wind speed along line A

Figure 17 and Figure 18 compare simulated speed up with measured values along line A. Speed-up results in both figures generally agree with measurements, and the result from QUICK scheme is a little better than the result from second order upwind discretization scheme. All simulations under predict the speed up at the site of HT, where the measured value is ΔS=0.88, simulations produce ΔS around 0.76. For the lee-side of the hill, Both simulations supper predict the speed up value, at a site on line A 400 meter's horizontally far from HT, the measured speed up value is ΔS=-0.65, Fluent simulations give ΔS from -0.50 to -0.52.

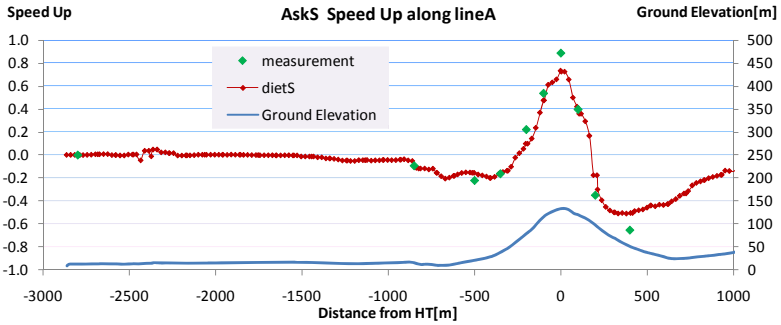

Figure 17. Comparison of measured and simulated velocity speed up along line A. Second-order upwind scheme. Calculated and measured speed ups are normalized with 8.979 and 8.6 m/s, respectively

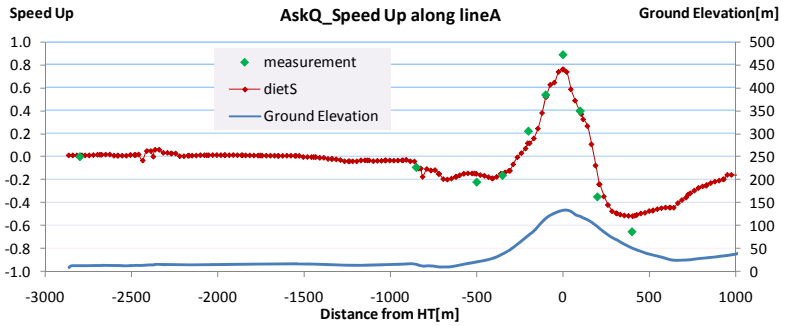

Figure 18. Comparison of measured and simulated velocity speed up along line A. QUICK scheme. Calculated speed up is normalized with 8.979 m/s *which is derived from inlet logarithmic profile at corresponding height, and measured speed up is normalized with 8.6* m/s.

Table 6. Speed up comparison of different simulation cases and measured values at two sites in line A-the highest point HT and the lee side point 400 m *from HT. Speed up are normalized with reference velocity 8.6* m/s. *Run AskS are results from Second order Up wind scheme, Run AskQ are results from QUICK scheme.*

Horizontal Distance from HT [m]	Speed Up			
	Measured value	Castro[8]	Fluent Simulation	
		RANS	AskS	AskQ
0	0.88	0.80	0.756	0.761
400	-0.65	-0.65 ~ -0.8	-0.50	-0.52

4.3.2 Turbulence kinetic energy along line A

The comparison of measured and simulated non-dimensional turbulence kinetic energy k/u^2 is shown in Figure 19, Figure 20. The simulated values are in good agreement with measurements along upstream and hill top points, except the lee-side point 400m from HT, due to the higher prediction of wind speed and lower prediction of turbulence kinetic energy, where the simulation with second order upwind scheme give a velocity of u=4.49 m/s and kinetic energy of k=4.36 m^2/s^2, while the measurement give u=3 m/s and k=4.29 m^2/s^2. The QUICK scheme produces a non-dimensional turbulence kinetic energy value for the last lee side point a little closer to measurement, with u=4.34 m/s and k=4.57 m^2/s^2.

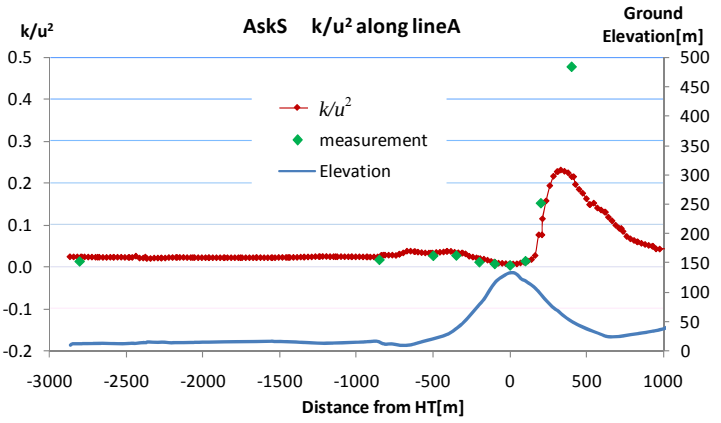

Figure 19. Comparison of measured and simulated non-dimensional $k^*=k/u^2$ along line A, this simulation applied second order upwind scheme.

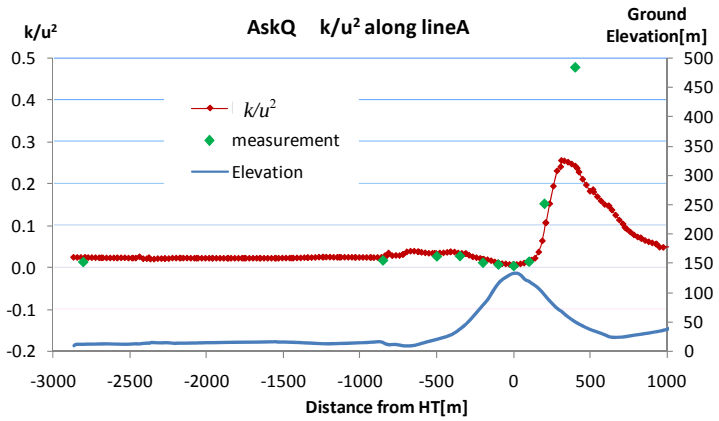

Figure 20. Comparison of measured and simulated non-dimensional $k^*=k/u^2$ along line A, this simulation applied QUICK scheme.

4.3.3 Wind speed distribution along line HT

Measurements and simulation results along line A suggested that the hill top point HT is best location for a wind turbine, where speed up is high and non-dimensional turbulence kinetic energy is relatively low. For wind power application, accurate prediction of wind speed around hub height of wind turbine is the most important. According to commonly available 1.0~2.5MW wind turbines, the concerned height will be higher than 10 meter and extend to 100 meter or higher. The calculated speed ups are nearly 10% smaller than measured values for the lower 4 points which are from 3 to 15 meter high but closely meet the higher two points, from 24 to 34 meter high (Figure 21 (*a*)). Our results are in accordance with Castro's simulation as well as other numerical and wind tunnel results referenced by Castro[8] (Figure 21 (*b*)), but a little closer to measurements. The results from second order up wind scheme and QUICK scheme are very close to each other.

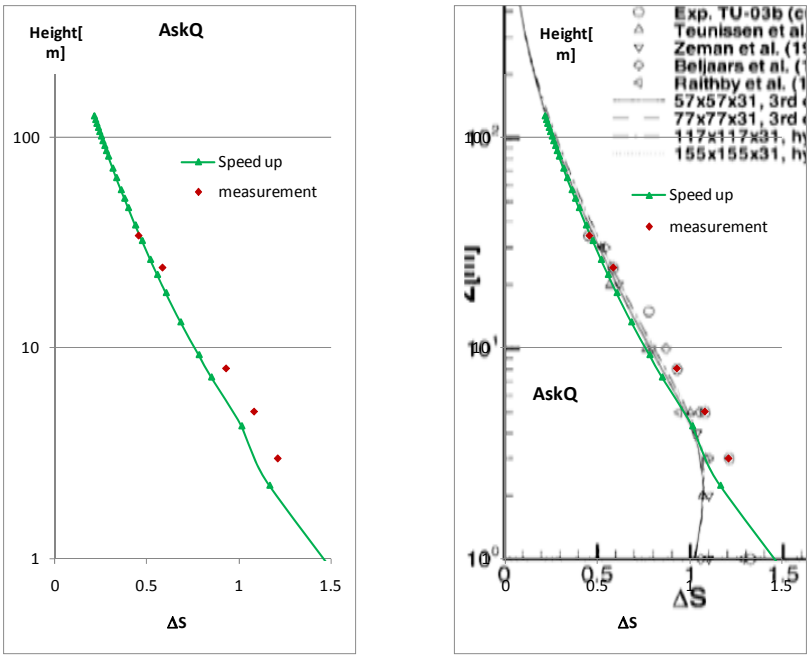

(*a*) (*b*)

Figure 21. Comparison of measured and simulated velocity speed up along vertical line HT. (a) measured speed up normalized with corresponding RS velocity, calculated speed up normalized with logarithmic equation (45) but for corresponding height above ground. (b) Compare with Castro's result.

4.4 Closure

Some key points of the Askervein Hill CFD simulation are as followings:

①Along upstream part of line A, mean wind speed up is well predicted.

②At top point of Askervein hill, 10 m above ground, simulated local absolute wind speed under predict measurement with about -3~-2% error, defined as (calculated velocity-measured velocity)/measured velocity, QUICK scheme produce a little better result than second order upwind scheme.

③Along line A, largest error happened at last measured point at lee side of the hill, with the best calculated speed up of -0.52 contrast to measured value -0.65.

④Except last point where velocity is supper predicted, non-dimensional turbulence kinetic energy are well predicted along line A.

⑤Along vertical line at HT, Simulation and measurements agree with each other. The calculated speed up lower predicted measurements at lower part, and is close to measurements at higher part, nearly identical to the highest point.

5 Simulation of a hat place terrain

Figure 22. Bolund hill, a small hill located north of Risø DTU, surrounded by sea water except a narrow, just above water road lead to land

Askervein hill is relatively smooth hill and cannot be classified as complex terrain, the wind field measurements was carried out some 25 years before, even the experiments produced plenty of data, measurements of some specific sites, especially lee side of the hill, are not enough. A new field measurement project was carried out during 2008 at Bolund hill (Figure 22), the measurement was designed with help of CFD simulation[19] and the measured data will be available in the mid of 2009. Bolund hill is about 12m high, 130m long and 75m wide, it is too small to represent a wind farm but very good for research work, especially for CFD and other wind power meteorological model's developing and verification. In this chapter we did not simulate the Bolund hill, as basic tool cases, we designed several hat place terrains as ideal, artificial Bolund hill. Just like a flat terrain simulation is good to verify and compare different models and codes, Simulation of a hat place will show some typical characteristics of the wind flow such as vortex and reverse flow, and it is good for comparison among different methodologies.

5.1 Problem description

One of the three hat terrains are shown in Figure 23. The hill is ellipse in plan form within a horizontal zone of 240 m on major axis and 170m in minor axis, a little larger than Bolund hill. Three terrains were simulated denoted as test1, test2 and test3, the first one looks like Bolund hill in side view and is the same 12m high. The second one is based on the first one with amplified height of 24m, and the third one is based on the first case with same height but smoother edge slope. The inlet boundary conditions for the three simulation cases are the same, wind direction is along the major axis of the elliptical hat. Figure 23 shows only the hat place of the domain, the simulation domain extend 1km upwind and downstream, respectively, and extend 500m toward both sides, the height of the simulation domain is 1.5km above surrounding ground, higher than the height of neutral ABL.

Table 7 Characteristics of the 3 simulated hat terrains

Simulation case	Test1	Test2	Test3
Hill height[m]	12	24	14
Brim slope	steep	steep	smoother

The artificial Bolund hill is a typical complex terrain problem with steep slope. We may image rotation of wind at upwind side, lee side and from both tangential sides at specific hill height, brim slope angle and coming wind speed. It is reasonable to anticipate that parameter gradients should be remarkable around and above the brim

slope. The first attention should be paid to meshing of simulation domain. At present, the ground is divided into 4 zones from centre to outer surroundings. The first zone is at top of the hat terrain with uniform altitude and elliptical outer borderline, major and minor axes are 160m and 80m, respectively. The adjacent second zone include all slope ring around the hill, altitude change from zero to hill height, it's major and minor axes of outer elliptical borderline are 250m and 180m, respectively. The third zone is from ellipse to square zone with outer square borderline's side length of 280m. The forth zone include all other flat ground surface and is subdivided into 8 sub-zones for meshing convenience. The meshing schemes for the first three zones are shown in Figure 23(*b*). The first zone is meshed with fine unstructured grid, the second zone is meshed with fine regular grid, the third zone is meshed with unstructured grid from inner fine to outer coarse, the forth zone is meshed with regular grid and applied a successive ratio scheme toward upwind and downstream directions to get a gradual change of grid size. The whole simulation domain is divided into different volume zones according to the partition of ground surface, and meshing along height direction apply same successive ratio scheme for each volume zone.

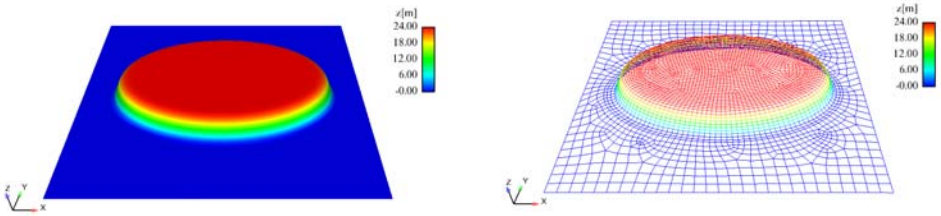

(*a*) (*b*)

Figure 23. Terrain for test2. (a) The hat place, (b) the mesh of the hat place and surrounding ground

For the inlet wind profile, we use a friction velocity of $u^* = 0.6183$ m/s, von-Karman constant is $\kappa = 0.4$, and aerodynamic roughness length is $z_0 = 0.03\,\mathrm{m}$. the inlet wind profile could be rewritten as

$$u = \frac{u^*}{\kappa}\ln\left(\frac{z}{z_0}\right)$$

$$k = \begin{cases} \dfrac{u^{*2}}{\sqrt{C_\mu}}\left(1-\dfrac{z}{Hg}\right)^2 & z < Hg \\ 0.0001 & z \geq Hg \end{cases}$$

$$\varepsilon = \frac{u^{*3}}{\kappa(z-2.998)}$$

Standard *k*-ε 2-equation viscous model is applied with modified model constants shown in Table 2. The user defined wall functions are applied for near wall treatment.

5.2 Simulation results

Figure 24 shows velocity vectors in a vertical section at windward side and leeward side of the hill. It could be seen that for the near foot zone of the hill, wind is slow down at both sides along wind direction. Both of them could be used to take shelter from wind, but the rear part is better than the front part, say, the shelter space is larger than front one. The wind is weak and rotating in these two zones.

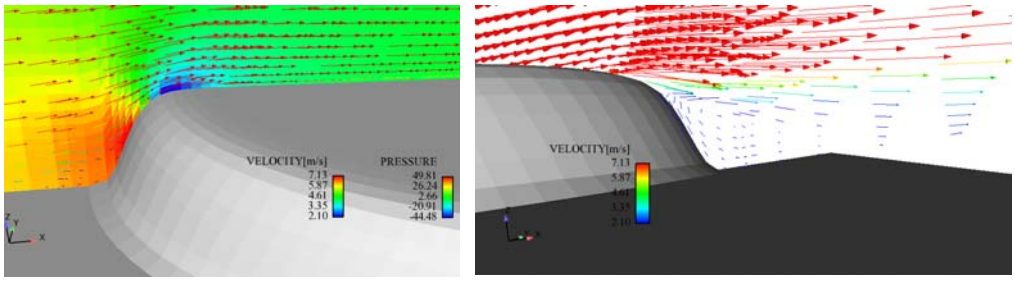

(*a*) (*b*)

Figure 24. Test2 velocity vectors in a vertical section at (a) upwind side and (b)lee side of the hat place

In order to compare simulation results, we chose three lines in same vertical section passing the major axis of the elliptical hill, with height to ground surface of 2m, 5m and 10m, respectively. These lines are marked as Z=2m, Z=5m and Z=10m, but note that the altitude of the line change with ground surface elevation.
Speed up along those lines for test1, test2 and test3 are shown in Figure 25, Figure 27 and Figure 29, respectively. It could be seen that in test1 with steep slope hill edge and 12m hill height, along the line 2m above ground surface, reversed wind speed appear at both windward and leeward sides of the hill, along the 5m and 10m lines no reversed wind speed appear. But in result of test2, reversed wind speed appear in leeward zone along all three lines, in windward zone, reversed speed only appear at 2m height. In result of test3, no reversed wind speeds appear along those lines.

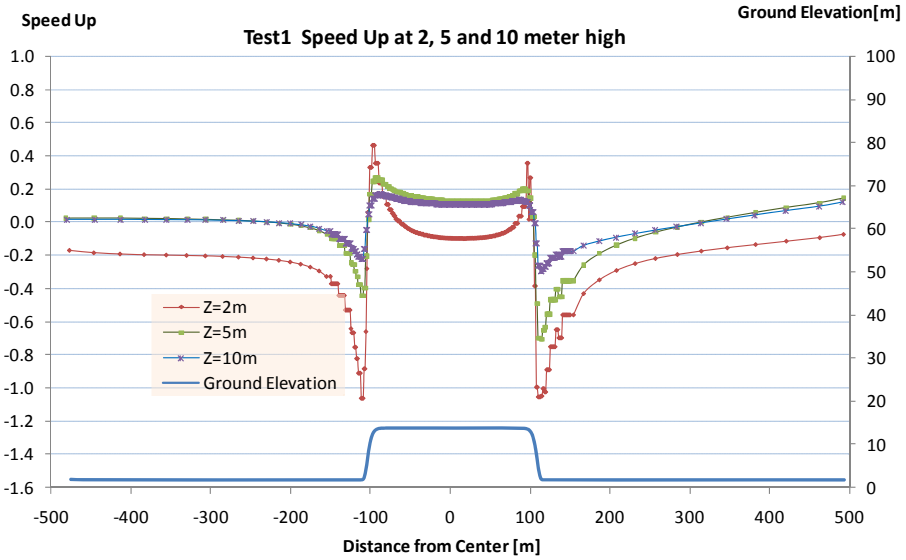

Figure 25. Normalized speed along x-direction lines at 2, 5, 10 meters high. Speed up is normalized with inlet velocity 6.49, 7.91, 8.98 m/s respectively

Along all three lines in all cases, wind speed will slow down approaching the slope, increase sharply at slope because it is steep, decrease first and then increase along top plane of the hat to the second peak approaching leeward slope, and then slow down sharply at down slope to second valley bottom, then increase gradually to it's

coming condition. Above the top plane of the hat, speed up is a 'saddle' curve, this curve shape agrees with measurements of Bolund hill qualitatively.
The simulated turbulence kinetic energy distributions along those three lines are shown in Figure 26 and Figure 28 for simulation test1 and test2, respectively.

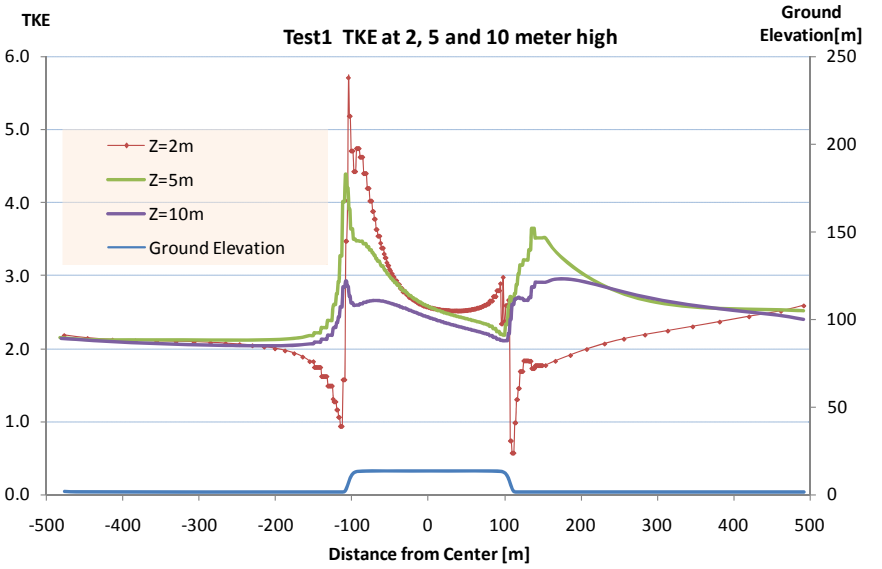

Figure 26. Turbulence kinetic energy along x-direction lines at 2, 5, 10 meters high.

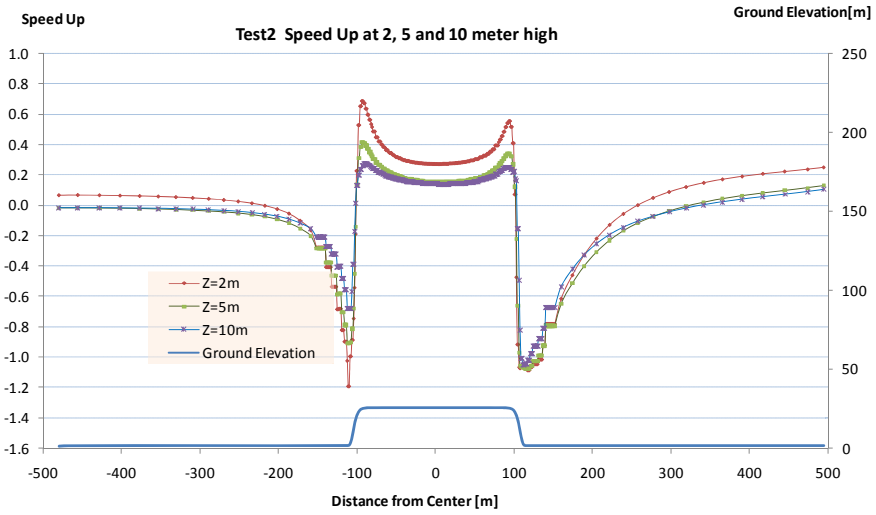

Figure 27. Normalized speed along x-direction lines at 2, 5, 10 meters high. Speed up is normalized with inlet velocity 6.49, 7.91, 8.98 m/s respectively.

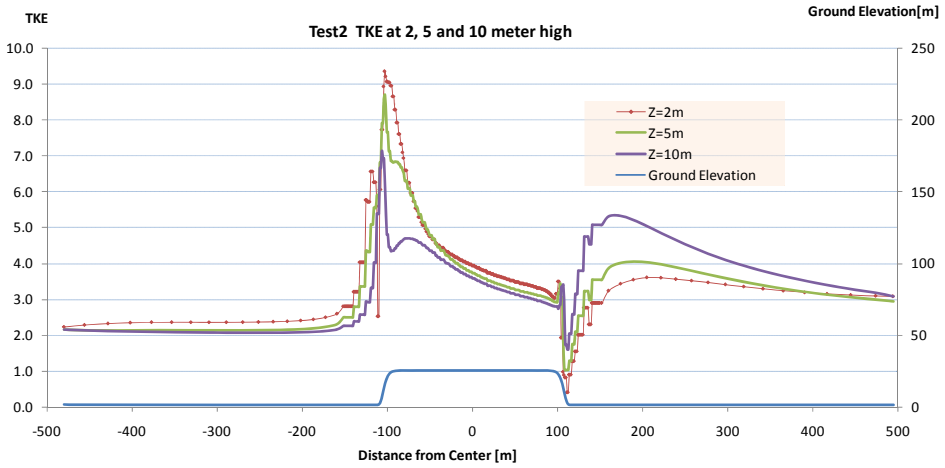

Figure 28 Turbulence kinetic energy along x-direction lines at 2, 5, 10 meters high.

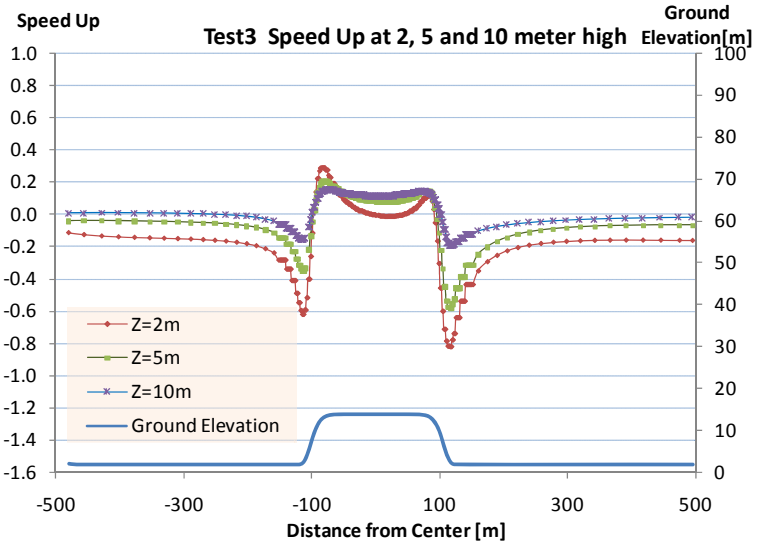

Figure 29. Normalized speed along an x-direction line at 2, 5, 10 meters high. Speed up is normalized with inlet velocity 6.49, 7.91, 8.98 m/s respectively

\

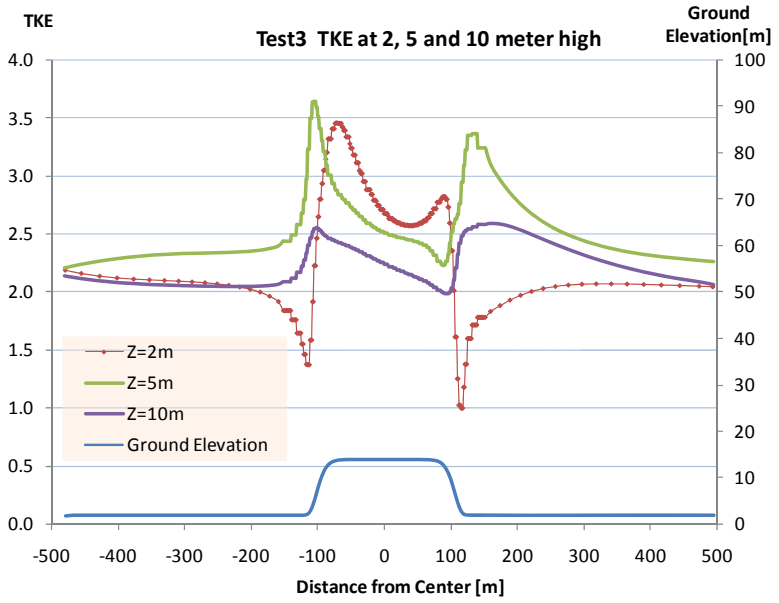

Figure 30. Turbulence kinetic energy along an x-direction line at 2, 5, 10 meters high above ground surface.

There are at least two problems in the simulation results. As mentioned in chapter 3, the present CFD model will not produce a perfect homogenous flow along flat terrain. Figure 11 show that there is negative velocity gradient at the bottom of the domain, say, under 10m high, but the change of speed up should be within 5%. The first problem comes from the 2m high lines before the hill. In test1 and test3, speed up is lower than zero but beyond 5%, in case of test2, speed up is higher than zero. It seems that the speed up along 2m high line is influenced by the hill and, maybe, the space extension of the simulated domain. For simulation case of test3, the smoother hill, the outlet speed ups are almost the same with inlet values, but for steep slope cases, test1 and test2, outlet speed ups are higher than inlet values, this is the second problem. Widen the simulation space may soft this problem.

Acknowledgements

Work in this report was carried out with direction and help of Andreas Bechmann, but the report represent only views of the author's.
Thanks to Niels N. Sørensen for his helpful suggestion and discussion, some research work in this report are base on his inspiration and advice. Thanks to Flemming Rasmussen for his arrangement of our work and kindly encouragements. Thanks to Jens Carsten Hansen for his help, it is based on his effort and fruitful work that the research could begin and go smoothly. Thanks to colleagues in Wind Energy Division for their kindness and help, Xiaodong zhang appreciate very much the working opportunity in Risø DTU as visiting scientist.

Reference

1. Bechmann, A., *Large-Eddy simulation of atmospheric flow over complex terrain.* science of making torque from wind, 2007. **27**.
2. Hanjalic, K. and S. Kenjeres, *Some developments in turbulence modeling for wind and environmental engineering.* Journal of Wind Engineering and Industrial Aerodynamics, 2008. **96**(10-11): p. 1537-1570.
3. Hargreaves, D.M. and N.G. Wright, *On the use of the k-epsilon model in commercial CFD software to model the neutral atmospheric boundary layer.* Journal of Wind Engineering and Industrial Aerodynamics, 2007. **95**(5): p. 355-369.
4. Brodeur, P. and C. Masson, *Numerical site calibration over complex terrain.* Journal of Solar Energy Engineering-Transactions of the Asme, 2008. **130**(3).
5. Blocken, B., T. Stathopoulos, and J. Carmeliet, *CFD simulation of the atmospheric boundary layer: wall function problems.* Atmospheric Environment, 2007. **41**(2): p. 238-252.
6. Blocken, B., J. Carmeliet, and T. Stathopoulos. *CFD evaluation of wind speed conditions in passages between parallel buildings - effect of wall-function roughness modifications for the atmospheric boundary layer flow*. in *4th European and African Conference on Wind Engineering*. 2005. Prague, CZECH REPUBLIC.
7. **Mandas N., C.F., Crasto G., Cau G.**, *Numerical simulation of the atmospheric boundary layer (ABL) over complex terrain*. **2004**, EWEC 2004,London.
8. Castro, F.A., J. Palma, and A.S. Lopes, *Simulation of the Askervein flow. Part 1: Reynolds averaged Navier-Stokes equations (k-epsilon turbulence model).* Boundary-Layer Meteorology, 2003. **107**(3): p. 501-530.
9. Kim, H.G., V.C. Patel, and C.M. Lee, *Numerical simulation of wind flow over hilly terrain.* Journal of Wind Engineering and Industrial Aerodynamics, 2000. **87**(1): p. 45-60.
10. Inc., F., *Fluent 6.3 user's guide*. 2006, Fluent Inc.
11. Richards, P.J. and R.P. Hoxey. *APPROPRIATE BOUNDARY-CONDITIONS FOR COMPUTATIONAL WIND ENGINEERING MODELS USING THE KAPPA-EPSILON TURBULENCE MODEL*. in *1st International Symp on Computational Wind Engineering (Cwe92)*. 1992. Tokyo, Japan.
12. Zdunkowski, W. and A. Bott, *Dynamics of the Atmosphere: A Course in Theoretical Meteorology*. 2003: Cambridge University Press.
13. Burton, T., *Wind Energy Handbook*. 2001: Wiley.
14. Bechmann, A., et al. *Hybrid RANS/LES method for high reynolds numbers, applied to atmospheric flow over complex terrain - art. no. 012054*. in *Conference on the Science of Making Torque from Wind*. 2007. Lyngby, DENMARK.
15. Kaimal, J. and J. Finnigan, *Atmospheric Boundary Layer Flows: Their Structure and Measurement*. 1994: Oxford University Press, USA.
16. Taylor, P.A. and H.W. Teunissen, *THE ASKERVEIN HILL PROJECT - OVERVIEW AND BACKGROUND DATA.* Boundary-Layer Meteorology, 1987. **39**(1-2): p. 15-39.
17. **Taylor, P.A., Teunissen, H.W.**, *ASKERVEIN 82: Report on the September/October 1982 Experiment to Study Boundary-Layer Flow Over Askervein, South Uist.*, in *Research Report MSRB-83-8*. 1983.

18. **Taylor, P.A., Teunissen, H.W.**, *The Askervein Hill Project: Report on September/October 1983 Main Field Experiment*, in *Internal Rep. MSRB-84-6,*. 1985.
19. Andreas, B., J. Jeppe, and S. Niels N, *The Bolund experiment-design of measurement campaign using CFD*. 2007, Risø National Laboratory.